Palaeontology The Palaeontological Association www.palass.org

[Palaeontology, 2022, e12597]

Feeding habits of the Middle Triassic pseudosuchian *Batrachotomus kupferzellensis* from Germany and palaeoecological implications for archosaurs

by EUDALD MUJAL[1,2], CHRISTIAN FOTH[3], ERIN E. MAXWELL[1], DIETER SEEGIS[1] *and* RAINER R. SCHOCH[1,4]

[1]Staatliches Museum f¨ur Naturkunde Stuttgart, Rosenstein 1, 70191 Stuttgart, Germany; eudald.mujalgrane@smnsw-bw.de, erin.maxwell@smnsw-bw.de, dieter.seegis@smnsw-bw.de, rainer.schoch@smnsw-bw.de
[2]Institut Català de Paleontologia Miquel Crusafont, ICTA-ICP building, c/ de les columnes s/n, 08193 Cerdanyola del Vallès, Catalonia, Spain
[3]Department of Geosciences, University of Fribourg, Chemin du Musée 6, 1700 Fribourg, Switzerland; christian.foth@gmx.net
[4]Fachgebiet Paläontologie, Institut für Biologie, Universität Hohenheim, Wollgrasweg 23, 70599 Stuttgart, Germany

Typescript received 5 August 2021; accepted in revised form 23 December 2021

Abstract: Bite traces on fossil bones are key to deciphering feeding ecology and trophic interactions of vertebrate past ecosystems. However, similarities between traces produced by different carnivorous taxa with similar dentitions, and misidentifications due to equifinality, hinder confident identifications of the bite makers. Here, we correlate bite traces with macroscopic wear and microanatomy of the teeth of the pseudosuchian archosaur *Batrachotomus kupferzellensis* from the Triassic Lower Keuper fossil lagerstätten (southern Germany), untangling its feeding habits and shedding light on the bite traces generated by ziphodont teeth (teeth with serrated carinae). Individually, bite traces reflect tooth morphology, whereas composite bite traces and their frequency are related to feeding behaviour and explain tooth macroscopic wear and microanatomy. Therefore the identification of the bite maker is possible by analysing composite bite traces, their location on bones, and their relative abundance. In addition, tooth macroscopic wear and microanatomy are proven as independent lines of evidence of feeding ecology. Comparing bite traces on fossil and present-day bone assemblages, we observe that bone modifications by the crocodylomorph lineage (from Triassic pseudosuchian archosaurs to extinct and extant crocodylians) are strikingly similar, including taxa with and without ziphodont teeth. Such a set of features differs from bone modification assemblages produced by taxa with similar ziphodont teeth outside the pseudosuchian lineage, such as theropod dinosaurs and the Komodo monitor, suggesting phylogeny is a better predictor of feeding ecology among saurian reptiles than tooth morphology.

Key words: bite traces ('bite marks'), ziphodont teeth, tooth macrowear, tooth histology, archosaur, Lower Keuper.

DIRECT evidence of feeding ecology and trophic interactions of fossil vertebrates mostly relies on the identification of bite traces on bones (Fiorillo 1991; Jacobsen 1998; Pobiner 2008; Drumheller *et al.* 2020), stomach contents and processed food in the form of coprolites and regurgitalites (Qvarnström *et al.* 2019; Gordon *et al.* 2020). Regarding bite traces, however, the identification of the producer (the bite maker) commonly remains impossible (Hone & Chure 2018) and can usually only be confidently identified at a major clade level (Mikuláš *et al.* 2006; Jacobsen & Bromley 2009; Pirrone *et al.* 2014; Augustin *et al.* 2020; Drumheller *et al.* 2020; Drymala *et al.* 2021). In addition, even if carcass utilization by carnivores is recognized, feeding habits may still remain uncertain (Hone & Rauhut 2010; Drumheller *et al.* 2014, 2020).

This is particularly the case for ziphodont teeth (teeth with serrated carinae; Brink *et al.* 2015) because this dentition evolved convergently in different amniote clades (Whitney *et al.* 2020) but produces similar bite trace morphotypes (D'Amore & Blumenschine 2009). Taxa with ziphodont teeth include archosauromorphs (mostly purported terrestrial carnivores, but also phytosaurs and some marine crocodylomorphs), *Varanus komodoensis* (the extant Komodo monitor) and gorgonopsian therapsids (D'Amore & Blumenschine 2009, 2012; Pirrone *et al.* 2014; Brink *et al.* 2015; Hone & Chure 2018; Whitney *et al.* 2020). Interpretations of feeding ecology and trophic interactions based on bite traces of extinct taxa with ziphodont teeth are often limited to non-avialan theropod dinosaurs (Fiorillo 1991; Jacobsen 1998; Jacobsen & Bromley 2009; Drumheller *et al.* 2020), with additional information obtained from bite traces produced by *V. komodoensis* (D'Amore & Blumenschine 2009, 2012).

doi: 10.1111/pala.12597

Here, based on the tetrapod collection from the Lower Keuper (Erfurt Fm., Ladinian, Middle Triassic) Kupferzell and Vellberg-Eschenau fossil lagerstätten, south-western Germany (Urlichs 1982; Schoch & Seegis 2016; Schoch *et al.* 2018), we reconstruct an exceptional palaeoecological scenario by combining multiple morphological and statistical analyses. We correlate the diverse bite trace assemblage with the macroscopic wear and microanatomy of the teeth of the up to five-metre-long pseudosuchian archosaur *Batrachotomus kupferzellensis* (Gower 1999; Gower & Schoch 2009), the bite maker of most of the traces studied herein. Since bite traces are confidently correlated to tooth macroscopic wear and therefore to microanatomical adaptations in tooth structure, our work shows that these can be independent lines of evidence to decipher feeding behaviours. With the aim of deciphering the feeding ecology behind bite traces produced by ziphodont teeth through morphological and statistical analyses, we show a linkage between bite makers' habits and phylogeny among archosaurs and, more broadly, saurian reptiles.

GEOLOGICAL SETTING

The fossil tetrapod bones studied in this work come from two different fossil lagerstätten, named Kupferzell and Vellberg-Eschenau (Fig. 1). These rich fossiliferous deposits correspond to the Untere Graue Mergel (UGM; lower Grey Marls), a unit within the upper part of the Lower Keuper facies from south-western Germany (Lettenkeuper, Erfurt Formation), of Ladinian (late Middle Triassic) age (Urlichs 1982; Schoch & Seegis 2016) (Fig. 1A). In south-western Germany, the Lower Keuper mainly consists of an alternating carbonate–siliciclastic succession 20–25 m thick deposited in an epicontinental platform overlying the marine carbonate Muschelkalk facies (Brunner & Bruder 1981). This system is part of the Central European Basin, and during the Lower Keuper deposition it was occasionally flooded by marine transgressions from the Tethys sea, whereas the main sedimentary inputs came from the northern palaeogeographic highs (Etzold & Schweizer 2005; Nitsch 2015*a*, 2015*b*). The UGM is an overall succession of mudstones and marlstones, with different layers and bonebeds well-characterized at both the Kupferzell and Vellberg-Eschenau localities (Urlichs 1982; Nitsch 2015*c*; Hagdorn *et al.* 2015; Schoch & Seegis 2016). This unit is embedded between two dolostone banks, which may also contain fossils (Hagdorn *et al.* 2015; Schoch & Seegis 2016; Mujal & Schoch 2020).

The two localities are stratigraphically equivalent, though some lithological differences exist (Fig. 1B). The UGM layers in Kupferzell mostly present green, yellow and brown colours, whereas those from Vellberg-Eschenau are mainly grey-greenish and occasionally brown. Nevertheless, the palaeoenvironments for both localities are similar, being interpreted as lacustrine systems with marine influence and/or connection to marine environments, as evidenced by the presence of stratigraphically close marine carbonate units, and the presence of marine fossils, such as bivalves and sauropterygian reptiles within the UGM (Urlichs 1982; Nitsch 2015*c*; Hagdorn *et al.* 2015; Schoch & Seegis 2016; Mujal & Schoch 2020; DS, EM, RRS, pers. obs.)

MATERIAL AND METHOD

Institutional abbreviations. MHI, Muschelkalkmuseum Hagdorn, Ingelfingen, Germany; SMNS, Staatliches Museum für Naturkunde Stuttgart, Stuttgart, Germany.

Fossil sampling and analyses

All prepared fossil material from the Kupferzell and Vellberg-Eschenau fossil lagerstätten (south-western Germany) housed in the SMNS and MHI collections was examined using a magnifying glass, a dissecting microscope, and lighting in different orientations, to identify bite traces (e.g. Blumenschine *et al.* 1996; D'Amore & Blumenschine 2009; Drumheller & Brochu 2014; Drumheller *et al.* 2020). Bite traces were systematically classified according to their morphology (ichnotaxonomy) following Mikuláš *et al.* (2006), Jacobsen & Bromley (2009) and Pirrone *et al.* (2014). In addition, equivalences of the identified ichnotaxa with the taphonomic terms coined by Binford (1981) and extensively used in the literature (e.g. Pobiner 2008; D'Amore & Blumenschine 2009; Njau & Gilbert 2016; Drumheller *et al.* 2020) are provided. Associations between bite traces and their orientation and location on bones were also surveyed. All of this information can be found in Data S1 (and Mujal *et al.* 2022). In taphonomic studies, bite/tooth traces are often named bite/tooth 'marks' but, since they are biogenic structures (i.e. ichnofossils or trace fossils), the term 'trace' is preferred, with use of the term 'mark' restricted to non-biogenic structures (Bertling *et al.* 2006; Mikuláš *et al.* 2006; Jacobsen & Bromley 2009; Vallon *et al.* 2015).

Bite traces produced by the dragging of denticles on the carinae of teeth (ichnotaxon *Knethichnus parallelum*) were measured on digital photos using ImageJ (v.1.52a) following D'Amore & Blumenschine (2012). Such measurements account for the maximum number of denticles per millimetre, allowing for the identification of the potential bite maker through comparisons with the tooth assemblage from the Lower Keuper (Schoch *et al.* 2018).

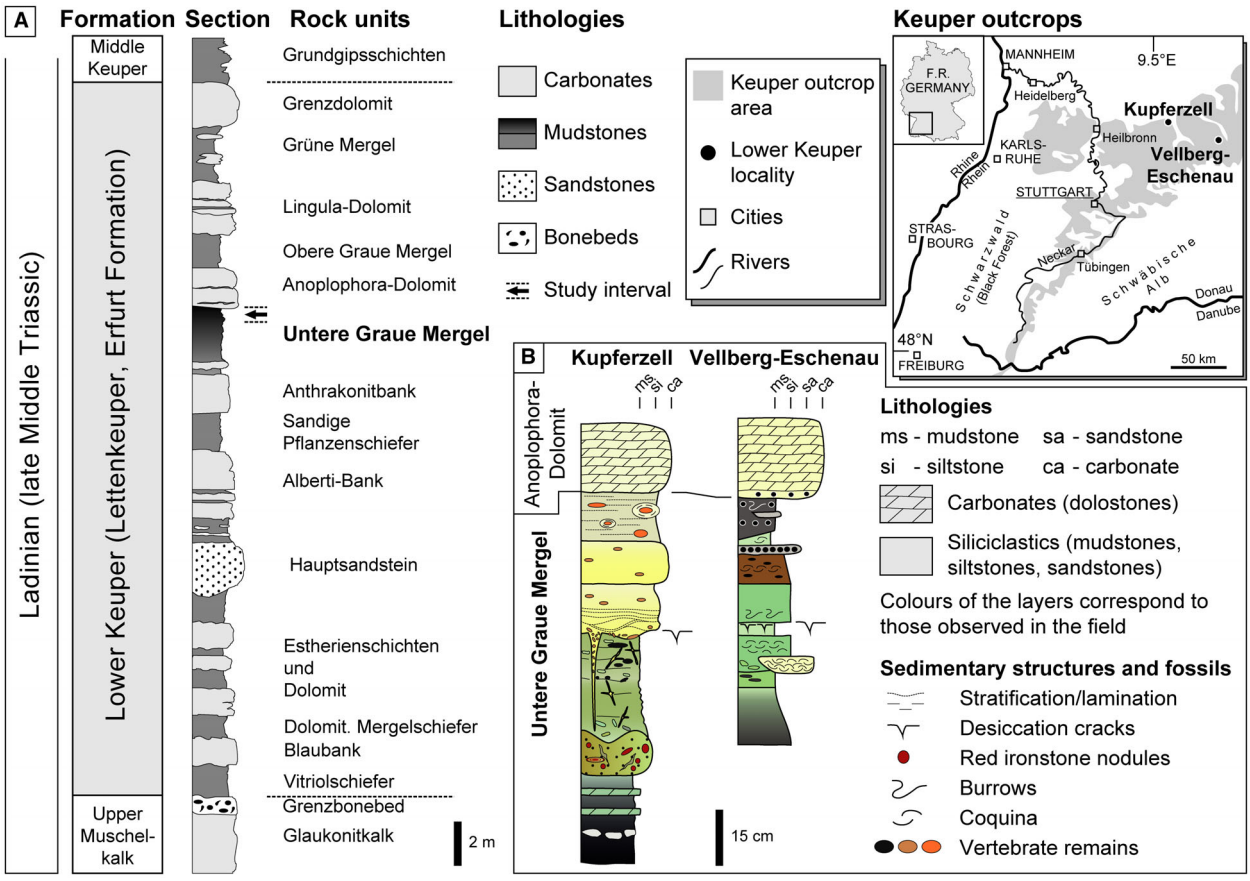

FIG. 1. Geological setting. A, general stratigraphic section and geological map of the Lower Keuper in south-western Germany (modified from Schoch & Seegis 2016; Schoch *et al.* 2018). B, detailed stratigraphic sections of the Kupferzell and Vellberg-Eschenau fossil lagerstätten (modified and updated from Hagdorn *et al.* 2015; Schoch & Seegis 2016).

Since most of the bite traces were assigned to *Batrachotomus kupferzellensis*, teeth of this pseudosuchian archosaur were analysed as explained below.

Tooth crowns of *Batrachotomus* from Kupferzell (N = 258) and Vellberg-Eschenau (N = 56), all from the UGM, were analysed accounting for: (1) basic morphological classification by measuring (with a digital calliper) the apicobasal height of the crown (or crown height, CH), the mesiodistal depth and the labiolingual width of the crown at its base (or crown base length, CBL, and crown base width, CBW, respectively; for tooth parameters, see: Smith *et al.* 2005; Hendrickx *et al.* 2015); (2) identification of the position within the jaw, distinguishing premaxillary from non-premaxillary teeth (also distinguishing teeth from the dentaries and maxillae, when possible). In order to identify the position of teeth within the jaws, we examined the dentigerous elements of *Batrachotomus* still preserving attached teeth and also followed tooth descriptions from Gower (1999) and Schoch *et al.* (2018). Generally, premaxillary teeth display distinctive features allowing them to be distinguished from those of the maxillae and mandibles. The premaxillae of *Batrachotomus* held four teeth each, these with a characteristic slender shape (Gower 1999). Teeth from the premaxilla were almost cylindrical, with a nearly round or slightly oval cross-section, and an apical portion which is slightly (linguo-)distally curved; their basal mesial carina often lacks denticles (Data S2). Non-premaxillary teeth generally show diverse crown morphologies (Gower 1999; Schoch *et al.* 2018), with differences in: (1) the distal curvature (symmetry in labial/lingual view); (2) the symmetry of cross-section (more or less convexity of the labial side, though all are oval in cross-section); (3) curvature towards the lingual side; and (4) relative height of the crown with respect to the mesiodistal depth of the crown base. Both mesial and distal carinae possess denticles. However, due to the isolated nature of most of the teeth, in most cases it was not possible to identify whether the non-premaxillary teeth were from the maxillae (with 11 alveoli each) or the mandibles (with probably 12 alveoli each) or from which tooth position. Only teeth still attached to maxillae or mandibles, as well as some teeth

with a recurved labial side of the crown and straight posterior edge that are characteristically from the anterior part of the maxilla (Gower 1999), can be more confidently positioned. According to Gower (1999, p. 38), teeth from the posterior part of the maxilla are more strongly convex anteriorly and have shorter crowns than those from the anterior part; however, these features seem to be present in some mandibular teeth. In addition, Schoch *et al.* (2018, p. 621) noted differences in tooth length across maxillae and dentaries, with the longest elements in the mid-portion of maxillae and anterior portion of dentaries and the smallest teeth in the anterior and posterior ends of maxillae. Nevertheless, the isolated nature of most of the teeth precludes their association to individuals, meaning that they could belong to either juvenile or mature/adult animals because teeth could be proportionally smaller or larger, respectively. Of note, all preserved dentigerous elements show that tooth replacement in *Batrachotomus* occurred at alternating tooth positions (Gower 1999).

Tooth macroscopic wear (macrowear) was classified in two ways (Table 1): qualitatively, distinguishing wear, notches, spalling and breakage, as well as noting the areas of the tooth crown with greater amounts of wear (lingual or labial, and mesial or distal); and (semi-)quantitatively, scoring the degree of tooth wear as none (0), low (1), high (2) or extreme (3). All tooth measurements and macrowear are integrated in Data S2 (see also Mujal *et al.* 2022). Based on the UGM tooth sample, we compared macrowear between premaxillary and non-premaxillary teeth in a box-plot by averaging the amount of macrowear (from none to extreme) of all teeth. In addition, we compared regional differences in macrowear (using averages) along the mesial and distal carinae and the tip in a box-plot. The number of occurrences (counts) of abrasion (wear and notches) for the tips and each portion of both mesial and distal carinae were counted and displayed as percentages for each region of the tooth crown, also differentiating between premaxillary and non-premaxillary teeth.

Tooth histology

To complement the interpretations based on the macroscopic wear of *Batrachotomus* teeth (see Discussion, below), we analysed their microanatomy, also comparing them to other taxa with ziphodont teeth (Brink *et al.* 2015; Wang *et al.* 2015; Whitney *et al.* 2020). Histological thin sections were prepared from isolated *Batrachotomus* teeth originating from the UGM and showing different degrees of macroscopic tooth wear. Four teeth (premaxillary: SMNS 97009/8; non-premaxillary: SMNS 97009/9, 97009/10, 97009/16), with one thin section each, were prepared in longitudinal section capturing either the mesial or distal carina. The crowns of two non-premaxillary teeth (SMNS 97009/11, 97009/17), with five thin sections each, were prepared in cross-section at varying points along the apicobasal axis. Thin sections were prepared following standard palaeohistological methodology, with thicknesses ranging from 60 to 75 μm, and examined under a petrographic microscope (Leica DM750P). Photographs were taken using an attached Leica ICC50 W camera, and processed using Leica LAS EZ (v.3.1.0) software.

Statistical analysis

To investigate potential statistical differences regarding bite trace patterns on different bitten taxa (*Mastodonsaurus* vs *Plagiosuchus* vs *Nothosaurus* vs *Batrachotomus*), body regions (skull vs teeth vs free vertebrae vs sacrum vs ribs vs pectoral girdle vs pelvic girdle vs limbs) and bone regions (proximal end vs distal end vs side (widest area) of the shaft vs edge (narrowest area) of the shaft vs bone edge vs bone centre), we converted the data collected in the bite trace database (Data S1) into three separate datasets, scoring the absence or presence of each bite trace morphotype for all bones within each group. A small fraction of bones were not included in the analyses (Data S1) because the elements could not be identified due to their fragmentary nature or preservation. These datasets were analysed using a permutational multivariate analysis of variance (PERMANOVA). This method estimates the potential overlap between two or more groups by testing the significance of their distribution on the basis of permutation (9999 iterations) and the Euclidean distance as distance measures. In contrast to parametric tests, PERMANOVA does not require normal distribution of the data (Anderson 2001; Hammer & Harper 2006). The spatial relationship between groups is expressed by an *F*-value and a Bonferroni-corrected *p*-value. Following Wills *et al.* (1994), the three datasets were further transformed into Euclidean distance matrices and subjected to a principal coordinate analysis (PCOA). This method reduces multivariate data down to a new set of independent variables (principal coordinates) that are linear combinations of the original set with zero covariance (Hammer & Harper 2006), providing a 'biting space'. Afterwards, we ran a broken-stick method for each PCOA to obtain the number of principal coordinates (PCOs) that contain the relevant amount of total variation (De Vita 1979; Jackson 1993). For these PCOs we applied a linear discriminant analysis (LDA), which reduces the number of PCOs to a smaller set of dimensions by maximizing the separation between the given groups using the Mahalanobis distance. This distance measure is estimated

TABLE 1. Types and amount of macroscopic wear as classified in this work.

Macroscopic wear types	Description	Amount of macroscopic wear		
		Low (1)	High (2)	Extreme (3)
Wear	Abrasion	Denticles still recognizable, only partially abraded	Denticles abraded to their base	Carina completely removed, abrasion extending beneath the interdental sulcus
Notches	Localized abrasion			
Spalling	Breakage of relatively small and thin conchoidal/oval-shaped flakes	Small flake/s detached, original tooth morphology still easily recognizable	Large flakes, covering a large portion of the tooth, but morphology still recognizable	Large flakes, covering a large portion of the tooth, morphology not recognizable
Breakage	Loss of tooth portions	As for spalling, but broken portions lack conchoidal/oval fractures		

Lack of wear is scored as none (0).

from the pooled within-group covariance matrix, resulting in a linear discriminant classifier and an estimated group assignment for each species. These results were cross-validated using Jackknife resampling (Hammer & Harper 2006; Hammer 2020). Based on the confusion matrix (Stehman 1997), we estimated the error of correct identification.

Finally, given that the microanatomy of *Batrachotomus* teeth is strikingly similar to that of other hypercarnivores with ziphodont teeth (see Microanatomy of *Batrachotomus* teeth, below), we statistically compared the overall tooth morphology or morphometry of *Batrachotomus kupferzellensis* with that of other archosauromorphs by combining our measurements with the data from Hoffman *et al.* (2019) on archosauromorph teeth and Hendrickx *et al.* (2015) on theropod teeth. Because both datasets include different sets of parameters, we restricted the comparison to the crown height (CH), crown base length (CBL), crown base width (CBW), number of denticles on the mesial mid-crown (MC) and number of denticles on the distal mid-crown (DC). The latter two parameters were measured for a subset of 23 teeth from the *Batrachotomus kupferzellensis* sample (Data S2). In addition, we created three ratios between CBL and CBW (CBR), CH and CBL (CHR), and MC and DC (MDCR). Specimens with incomplete measurements were excluded from the final dataset. All measurements and ratios were log-transformed and analysed with LDA (including Jackknife resampling) and PERMANOVA (with 9999 iterations and Bonferroni-correction for *p*-values). In addition, we ran the LDA with all *Batrachotomus* teeth grouped as 'unknown' and classified them based on the training set, including the remaining specimens from the two original datasets. All statistical analyses and ordination methods were performed with the program PAST v.4.03 (Hammer *et al.* 2001).

RESULTS

Description of bite trace morphotypes on Lower Keuper bones

The presence of bite traces on Lower Keuper bones has previously been mentioned (Wild 1978, 1979, 1980; Schoch & Seegis 2016) but never analysed in detail. A total of 189 bones and teeth (178 from Kupferzell and 11 from Vellberg-Eschenau), all from the Untere Graue Mergel (UGM; Wild 1980; Urlichs 1982; Schoch & Seegis 2016), yield at least one bite trace (Data S1). Bite traces are preserved on bones of *Mastodonsaurus* (N = 141), *Plagiosuchus* (N = 5), *Nothosaurus* (N = 2), ?Chroniosuchidae (N = 1), and *Batrachotomus* (N = 40). Since bite traces are trace fossils (Bertling *et al.* 2006; Pirrone *et al.* 2014; Vallon *et al.* 2015), they are ichnotaxonomically classified. We identified five bite trace morphotypes referred to previously described ichnotaxa (Mikuláš *et al.* 2006; Jacobsen & Bromley 2009) (Figs 2–6; Data S1): *Nihilichnus nihilicus*, round/oval punctures produced by tooth tips; *Linichnus serratus*, linear grooves with serrated margins produced by serrated carinae; *Knethichnus parallelum*, regular and parallel grooves produced by denticles of carinae; *Brutalichnus* (two morphotypes), large holes reaching cancellous bone indicating strong bites; and *Machichnus*-like, multiple small punctures connected with short grooves produced by relatively small teeth.

Ichnotaxon Nihilichnus nihilicus *Mikuláš* et al., *2006.* Circular to oval-shaped or fusiform trace that may perforate the bone cortex ('punctures' of Binford 1981 and D'Amore & Blumenschine 2009), destroying it and penetrating the cancellous bone (Fig. 2A, F, J). Alternatively, the tooth may just incise the bone ('pits' of Binford 1981

and D'Amore & Blumenschine 2009), bending and pressing the bone cortex into the spongiosa or superficially breaking it into flakes that remain in adherence with one another and with the spongiosa; in some cases depressing fractures are present due to the collapse of the bone surrounding the tooth impact area (Drumheller & Brochu 2016). Both circular and oval traces are considered to be *N. nihilicus*, independent of degree of penetration into the bone. Nonetheless, the notably shallower bite traces are here termed 'pits' (as in Binford 1981 and D'Amore & Blumenschine 2009) to distinguish them from the more penetrating ones, as they may represent different behaviours of the bite maker (mostly linked to the strength of the bite). Within the area contacted by the tooth, the cortical bone is usually concentrically fractured, with radial fractures accommodating the displaced fragments within the bone. In traces with an oval outline (usually with pointed ends), the displaced portion of the bone is symmetrically broken and displays a more depressed, central, straight ridge dividing the bitten area in two; they correspond to 'bisected pits', produced by laterally compressed teeth (e.g. D'Amore & Blumenschine 2009; Njau & Gilbert 2016; Drymala *et al.* 2021). If the (fractured) cortical bone is still attached in the bite impact area, it displays a main straight fracture running along the long axis of the trace, with concentric fractures outlining the bitten area. In extreme cases, the bite results in the formation of a sharp, deep, hole that penetrates the bone (but without mixing cortical and cancellous bone) and preserves the transverse outline of the biting tooth, of fusiform shape due to the tooth carinae (Fig. 2A), allowing its shape, and thus the bite maker, to be identified (Drumheller *et al.* 2014) (see Identification of the bite maker, below). This bite trace morphotype would result from the tooth tip piercing the bone (Mikuláš *et al.* 2006; D'Amore & Blumenschine 2009), mostly with a vertical movement of the tooth towards the bone in the direction of the crown longitudinal axis. All traces with this outline on the Lower Keuper bones fit with teeth of *Batrachotomus kupferzellensis*.

Ichnotaxon Linichnus serratus *Jacobsen & Bromley, 2009.* Traces composed of linear grooves with characteristic serrated margins and a U- or V-shaped transverse section on the cortical bone (Fig. 2A–C, E). They are equivalent to the 'furrows', 'scores' and 'edge marks' of D'Amore & Blumenschine (2009) (see also Bindorf 1981). The 'dental hacks' described by Jacobsen & Bromley (2009) may also correspond to short *Linichnus*, and are likely to be equivalent to 'edge marks'. Nomenclatural differences rely on the extension of the bite trace (from a few mm to up to 2 cm long) and the incision into the bone (i.e. just deforming or completely removing the cortical bone), as occurs with *Nihilichnus*; thus, even if all of these linear grooves correspond to the same ichnotaxon the markedly shallower traces, although classified as *Linichnus*, are termed 'scores' (as in D'Amore & Blumenschine 2009). The traces of *L. serratus* within the Lower Keuper assemblage range from short (2–3 mm; 'simple dental hacks' of Jacobsen & Bromley 2009) to relatively long (*c.* 1 cm, and up to 2 cm) grooves that are usually straight to slightly curved; they can display short striations parallel to the main groove. This trace is formed by the serrated cutting edge of the tooth crown (i.e. from teeth possessing denticles on the carinae) and/or the dragging of the (serrated) tooth tip on the bone (D'Amore & Blumenschine 2009; Jacobsen & Bromley 2009; Pirrone *et al.* 2014), with the tooth moving parallel to the longitudinal axis of the crown; in other words, the carina (usually the mesial but occasionally the distal; see Discussion, below) is the main portion of the tooth tracing the bone.

Ichnotaxon Knethichnus parallelum *Jacobsen & Bromley, 2009.* Traces consisting of sets of parallel striations resulting from dragging of the denticles of teeth carinae on the bone surface (D'Amore & Blumenschine 2009, 2012; Jacobsen & Bromley 2009; Pirrone *et al.* 2014) (Fig. 2A, B, D–I). They are very characteristic traces exclusively produced by ziphodont teeth, equivalent to the 'striated marks' and 'striated furrows' of D'Amore & Blumenschine (2009). In the Lower Keuper assemblage, sets of parallel striations can be several centimetres long (up to 3.5–4 cm; Fig. 2G). They are either rectilinear, gently arched or markedly curvilinear and/or sinuous (the latter resembling the 'hook marks' produced by crocodylians, see Njau & Gilbert (2016), even though their tooth carinae do not possess denticles); also, a single trace can be rectilinear in one part and become strongly curved in the other part (as do some 'striations with internal striae' produced by crocodylians; Njau & Gilbert 2016). They are in groups of 3 to up to 13 parallel striations, though this number can vary also in a single trace, reflecting the changing number of denticles in contact with the bone as a result of the curvature of the tooth carinae and/or the bone. This morphotype results from the transverse to oblique movement of the tooth along the bone (D'Amore & Blumenschine 2012), thus, the movement is perpendicular to oblique with respect to the longitudinal axis of the tooth crown (i.e. the movement is mostly perpendicular to that producing *Linichnus serratus*).

Ichnotaxon Brutalichnus *Mikuláš* et al., *2006.* Traces corresponding to relatively large holes due to the removal of portions of both cortical and cancellous bone. This ichnogenus is recorded by two clearly differentiated

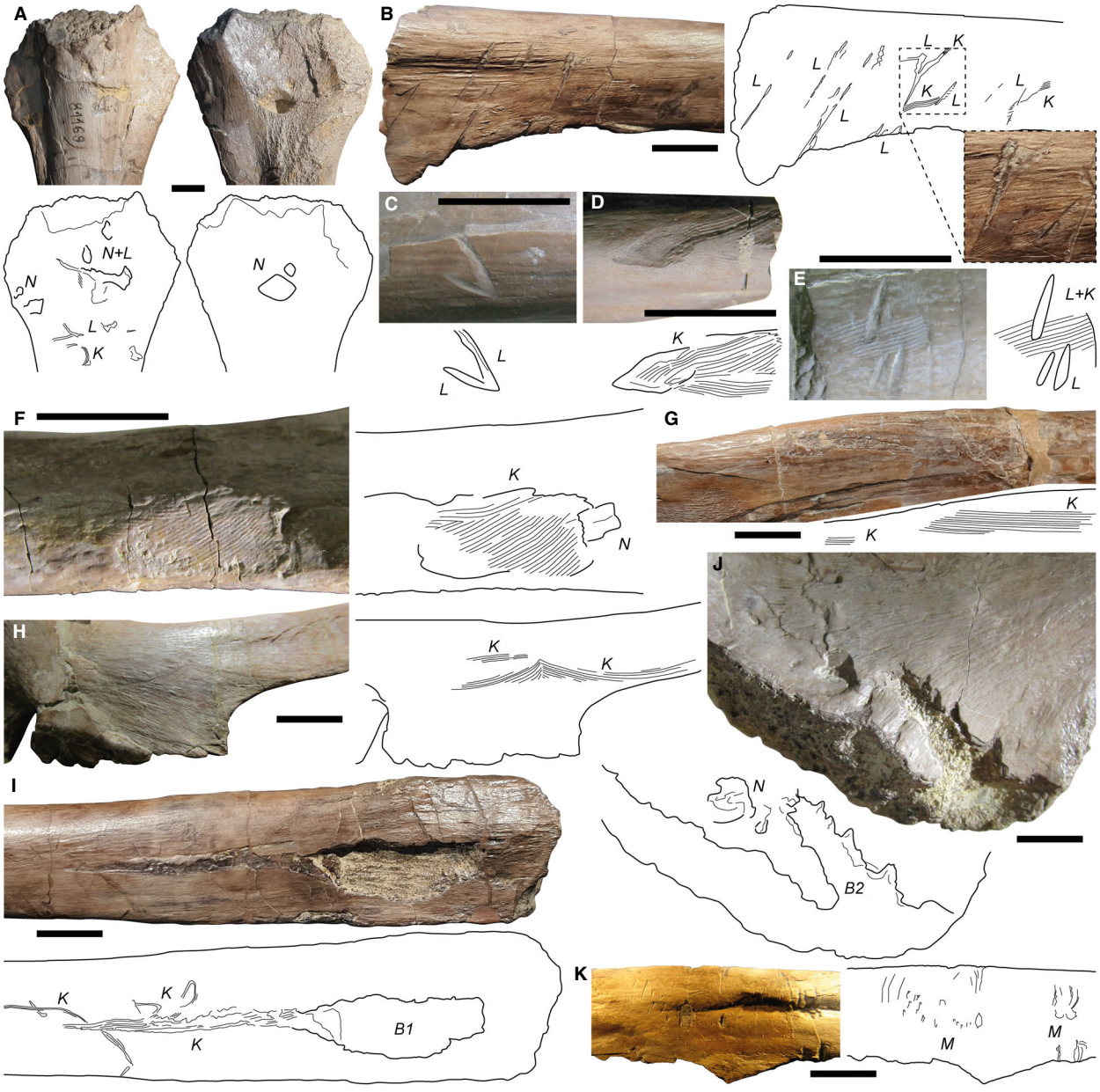

FIG. 2. Selected bite traces on Lower Keuper bones and interpretative outlines. A, punctures, grooves and drags on opposing surfaces (dorsal, left; ventral, right) of a right femur proximal end. B, aligned and N/Z-shaped traces on a right rib. C, V-shaped trace on a rib. D, pivoting drag trace within a rhomboid-shaped flake on a rib. E, associated grooves and drags on a right fibula. F, drag trace within a deep flake and puncture on a right radius. G, elongated drag trace on a left ischium. H, fan-shaped drag trace on a rib. I, curved and linear drag traces and deep trace on a right rib. J, V/triangular-shaped deep trace and punctures on an ischium. K, multiple small traces on a rib. A–B, F, I–J, *Mastodonsaurus*: SMNS 81169 (A), 97010/1 (B, I), 84256 (F), 84244 (J). C–E, G, K, *Batrachotomus*: SMNS 97013/1 (C), 97013/2 (D), 80277 (E), 80268 (G), 97014 (K). H, ?Chroniosuchidae: SMNS 97012. *Abbreviations*: *B1/B2*, *Brutalichnus* morphotypes 1/2; *K*, *Knethichnus parallelum*; *L*, *Linichnus serratus*; *M*, *Machichnus*-like; *N*, *Nihilichnus nihilicus*. All scale bars represent 10 mm.

morphotypes, here named morphotypes 1 and 2. The first one consists of relatively large and deep round to oval-shaped holes removing the cortical bone entirely and reaching the spongiosa (Fig. 2I). The second morphotype is represented by deep and elongated traces (also entirely removing the cortical bone) widening towards the edge of the bone, outlining a triangular- or V-shaped trace (Fig. 2J). The margins are roughly

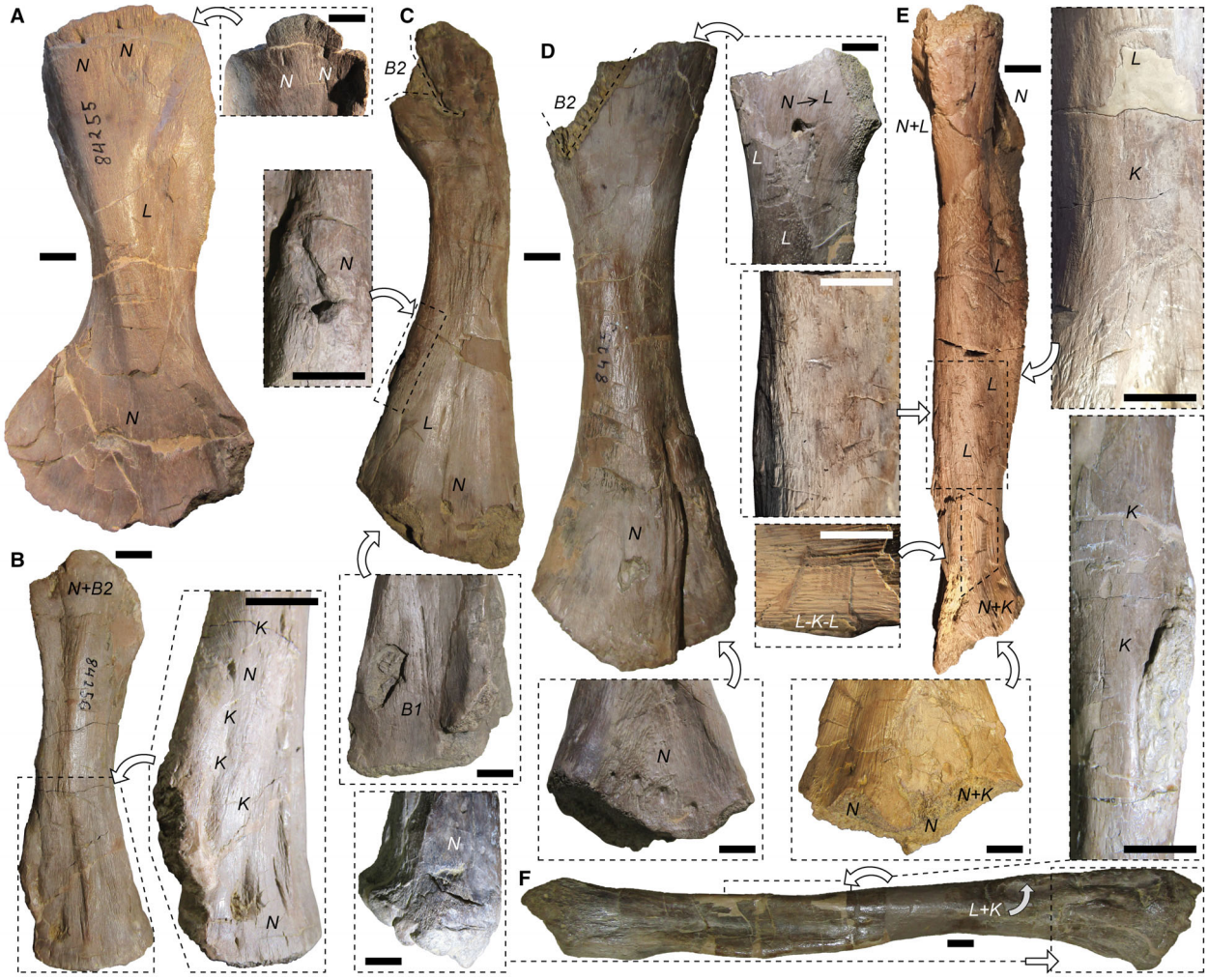

FIG. 3. Distribution of bite traces on bones from the Lower Keuper 1. A, right humerus with punctures on both ends and grooves on the shaft. B, right radius with punctures and deep traces on both ends and abundant drag traces on edge of the shaft (drag trace and puncture on the top of the inset photograph in B are shown in Fig. 2F). C–E, femora severely bitten, displaying diverse ichnotaxa and composite traces (proximal end of E shown in Fig. 2A). F, right fibula with puncture on the distal end, and long and thin drag traces on mid-shaft; arrow with *L+K* indicates position of traces shown in Figure 2E (on the opposite side, not visible in this image). A–E, *Mastodonsaurus*: SMNS 84255 (A), 84256 (B), 81361 (C), 84253 (D), 81169 (E). F, *Batrachotomus*: SMNS 80277. White arrows indicate position of enlarged images. *Abbreviations*: *B1/B2*, *Brutalichnus* morphotypes 1/2; *K*, *Knethichnus parallelum*; *L*, *Linichnus serratus*; *M*, *Machichnus*-like; *N*, *Nihilichnus nihilicus*. All scale bars represent 10 mm.

serrated; sometimes fracture lines which are concentric to the area of impact, and depressed fractures (Drumheller & Brochu 2016) are present. In both morphotypes, cortical bone may be still embedded (mixed) with cancellous bone within the deep holes. To generate the second morphotype, apart from the stark bone perforation, the tooth would also have been forcibly pulled back, ripping off the bone. This ichnotaxon probably resulted from a strong stroke of the bite-maker on the bone, possibly for the purpose of feeding on the marrow (Mikuláš *et al.* 2006), though considering the distribution of these traces in the Lower Keuper bones, this bite morphotype may also have resulted from dismembering or ripping off portions of the carcass.

Ichnotaxon Machichnus *(*Machichnus*-like) Mikuláš* et al.*, 2006.* Traces characterized by relatively small (1–2 mm long) hacks (in the sense of Jacobsen & Bromley 2009) found in abundance and aligned when present (only three bones bear this type of bite trace; Data S1) (Fig. 2K). The traces, which only affect the cortical bone, consist of small pits or punctures associated with a relatively short and straight groove with a pointed end, which may

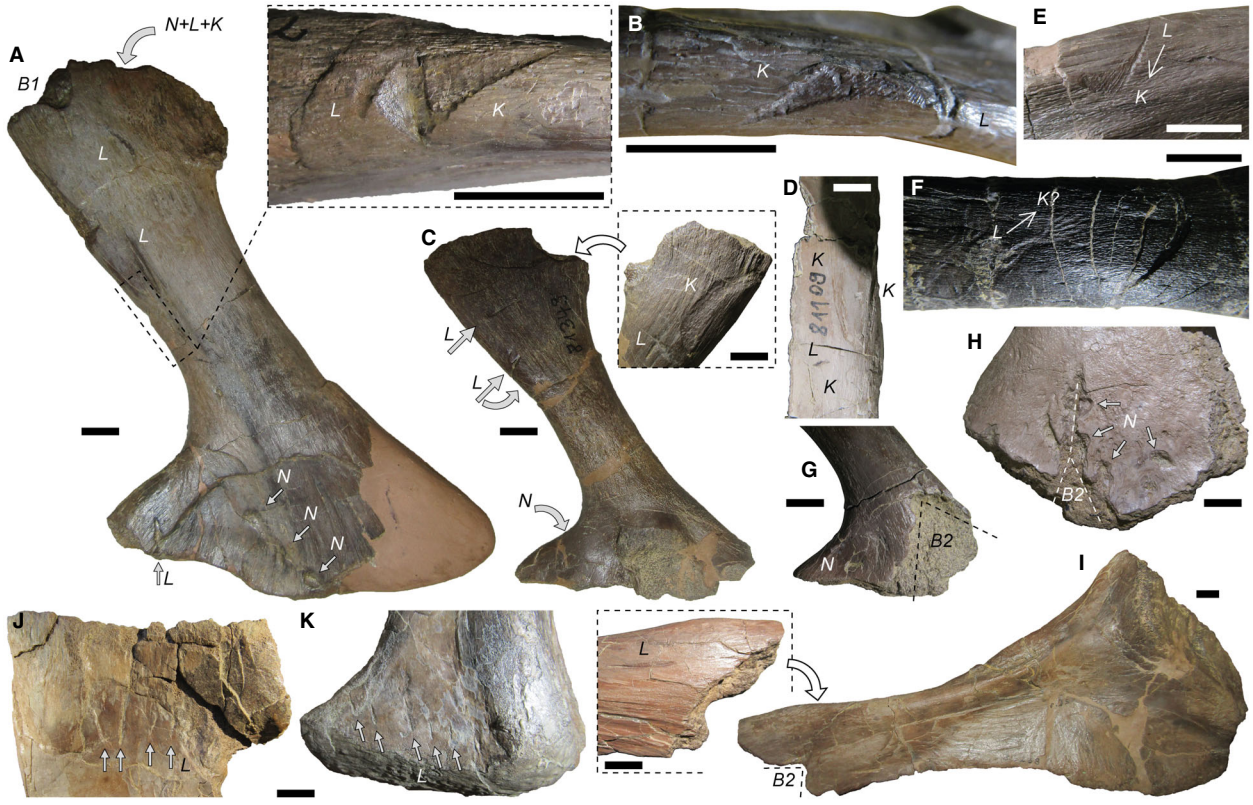

FIG. 4. Distribution of bite traces on bones from the Lower Keuper 2. A, ilium severely traced. B, edge of the shaft of a rib with a deep diamond-shaped flake displaying drag traces as in the inset of A. C, ilium with a deep flake as in the insets of A and B. D, rib with shallow drag traces outlining the same tooth movement as the flake with drags in C. E, rib with a transitional trace from groove to drag, showing the removal of a flake of bone with denticles dragged within. F, ilium with a groove potentially in transition with dragged denticles. G, ilium proximal end with a V-shaped deep trace and puncture. H, ischium (opposing side of this bone is shown in Fig. 2J) with a V-shaped trace and four aligned punctures fitting with the outline of a medium-sized *Batrachotomus* premaxilla. I, right ischium (pair of that of Fig. 2G) with a V-shaped trace and a linear groove (inset). J–K, proximal (J) and distal (K) ends of a right pubis with parallel grooves. A–E, G–H, *Mastodonsaurus*: SMNS 81342 (A), 81104 (B), 81349 (C), 81109 (D), 97010/2 (E), 81355 (G), 84244 (H). F, *Plagiosuchus*: SMNS 92055. I–K, *Batrachotomus*: SMNS 80268 (I), 52970 (J–K). Transitions between ichnotaxa are also observed (thin arrows between letters). *Abbreviations*: *B1/B2*, *Brutalichnus* morphotypes 1/2; *K*, *Knethichnus parallelum*; *L*, *Linichnus serratus*; *M*, *Machichnus*-like; *N*, *Nihilichnus nihilicus*. Large white arrows indicate position of magnified images; straight grey arrows indicate bite traces; curved grey arrows indicate position of trace on opposite side of element. All scale bars represent 10 mm.

occasionally result in a T-shaped trace. Some grooves display serrated margins, indicating that they were produced by (small) serrated teeth. In its diagnosis, this ichnotaxon was interpreted as a result of gnawing (Mikuláš *et al.* 2006) but, considering the specimens reported herein, it would more broadly represent repeated strokes on the bone. Interestingly, a 'gnawing-like' behaviour has recently been reported in a small-bodied theropod dinosaur (Brown *et al.* 2021); the bite traces reported herein (also associated with a small-bodied tetrapod, probably an archosauriform; see Identification of the bite maker, below) may represent a similar behaviour. In any case, considering the potential high disparity of behaviours (and wide range of potential bite makers), the bite traces of the Lower Keuper with this morphology are referred to as *Machichnus*-like, as the identification of this ichnotaxon is tentative.

Associations of bite traces from the Lower Keuper

All the previously described biting ichnotaxa are associated, with traces from the same and from different morphotypes, and show gradual transitions between types or are found in association with each other (being produced by the same taxon and/or individual; Figs 2A–J, 3–5; Data S1), with the exception of the *Machichnus*-like traces (Figs 2K, 6). The analysed bones

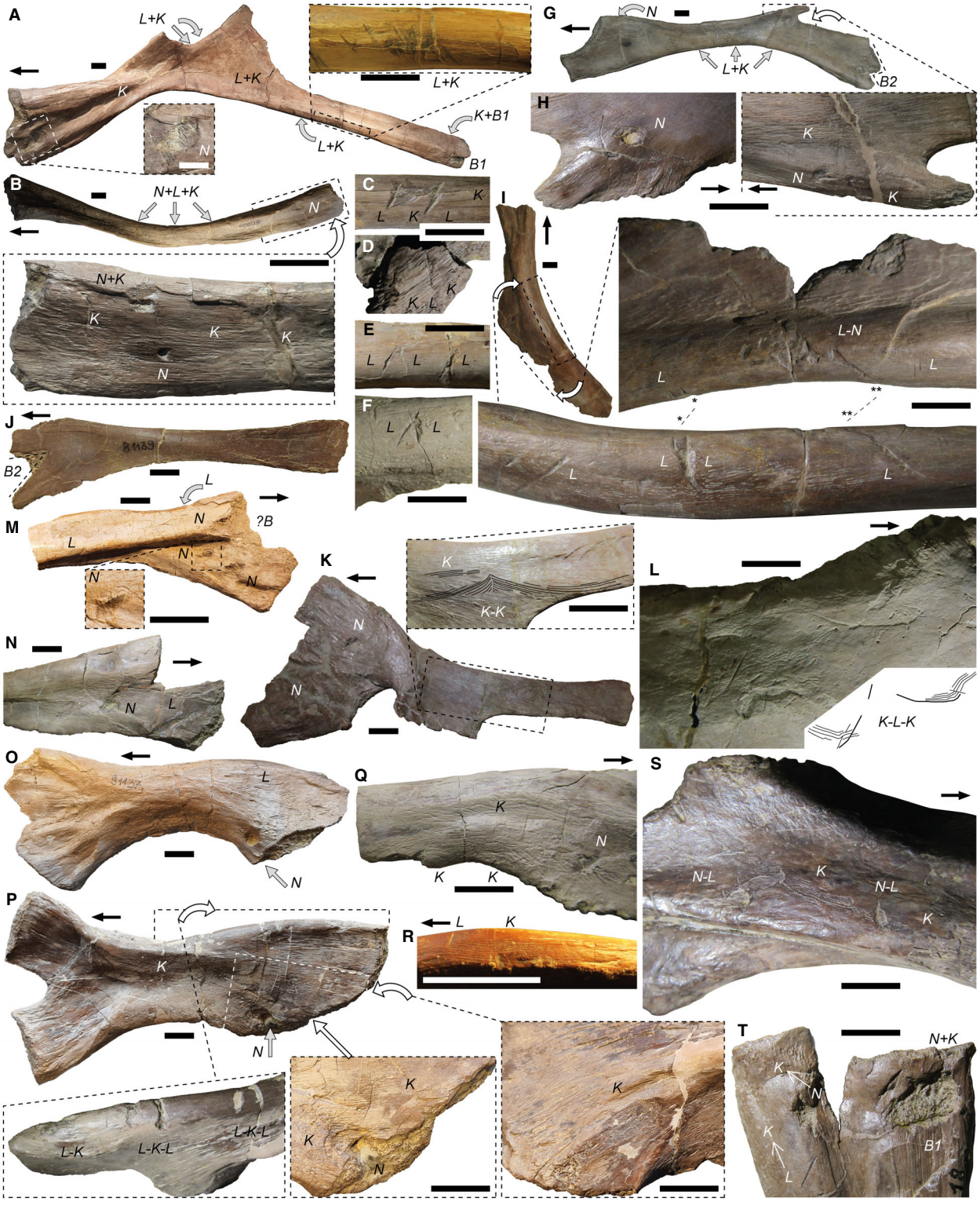

usually preserve several bite traces, in contrast to typical non-avialan theropod-traced bone assemblages (Fiorillo 1991; Jacobsen 1998; Pobiner 2008; Hone & Rauhut 2010; Augustin *et al.* 2020; Drumheller *et al.* 2020).

The most common association is a transition from *Linichnus* to *Knethichnus*, the long axes of each trace morphotype being perpendicular to oblique from each other (Fig. 2B, E). Transitions between *Linichnus* and

FIG. 5. Distribution of bite traces on bones from the Lower Keuper 3. Severely bitten bones corresponding to ribs (A–K, M–T) and a left cleithrum (L). A–D, F–J, L–M, O–Q, S–T, *Mastodonsaurus*: SMNS 97010/1 (A; traces on dorsal side of the shaft and end of rib shown in Fig. 2B, I), 80938 (B), 97010/3 (C), 84188 (D), 97010/4 (F), 81104 (G), 80915 (H), 80923 (I), 81139 (J), 81210 (L), 81123 (M), 81137 (O), 81136 (P), 97010/5 (Q), 97010/6 (S), 82018 (T). E, N, *Batrachotomus*: SMNS 97013/3 (E), 97013/4 (N)). K, ?Chroniosuchidae: SMNS 97012. R, *Nothosaurus*: SMNS 80266. Black arrows point to the proximal ends of bones. Transitions between ichnotaxa are also observed (thin arrows and hyphens between letters). *Abbreviations*: *B1/B2*, *Brutalichnus* morphotypes 1/2; *K*, *Knethichnus parallelum*; *L*, *Linichnus serratus*; *M*, *Machichnus*-like; *N*, *Nihilichnus nihilicus*. Large white arrows indicate position of magnified images; straight grey arrows indicate bite traces; curved grey arrows indicate position of trace on opposite side of element. All scale bars represent 10 mm.

FIG. 6. Bite traces not produced by *Batrachotomus* on Lower Keuper bones. Bitten bones of *Mastodonsaurus* (A–D) and *Batrachotomus* (E–F). A, palate (SMNS 80704) in ventral view with close up (dashed black square) of the paired *Nihilichnus*. B, mandible (SMNS 92128) with paired *Nihilichnus* similar to those in A. Dashed grey circles in A and B outline the approximate shape of the biting teeth (probably a pair of tusks of *Mastodonsaurus*). C, palate (SMNS 81310) with slightly sinuous scores (grooves) without serrated margins, differing from those produced by teeth with serrated carinae (i.e. generating the ichnotaxon *Linichnus serratus*). D, left cleithrum (SMNS 81210) with small cluster of *Machichnus*-like traces on the left part of the photograph, and *Knethichnus parellelum* pointed with an arrow and '*K*' on the right (see Fig. 5L). E–F, rib (SMNS 97013/5) with abundant *Machichnus*-like traces parallel to each other and with grooves (some with serrated margins) perpendicular to the rib long axis. Scale bars represent: 100 mm (A); 10 mm (inset of A, B–F).

Knethichnus (e.g. Figs 2B, E, 3E, 4E) indicate that the tooth tracing the bone changed its direction of movement. Usually, in this composite trace, the length of *Linichnus* is greater than the width of *Knethichnus* (the latter corresponding to the set of parallel striations generated by the denticles). This composite trace is somewhat similar to the bone spalling inferred for crocodylian-induced bite traces (Njau & Gilbert 2016). Several bones preserve an association of *Linichnus–Knethichnus–Linichnus*, with two parallel *Linichnus* and

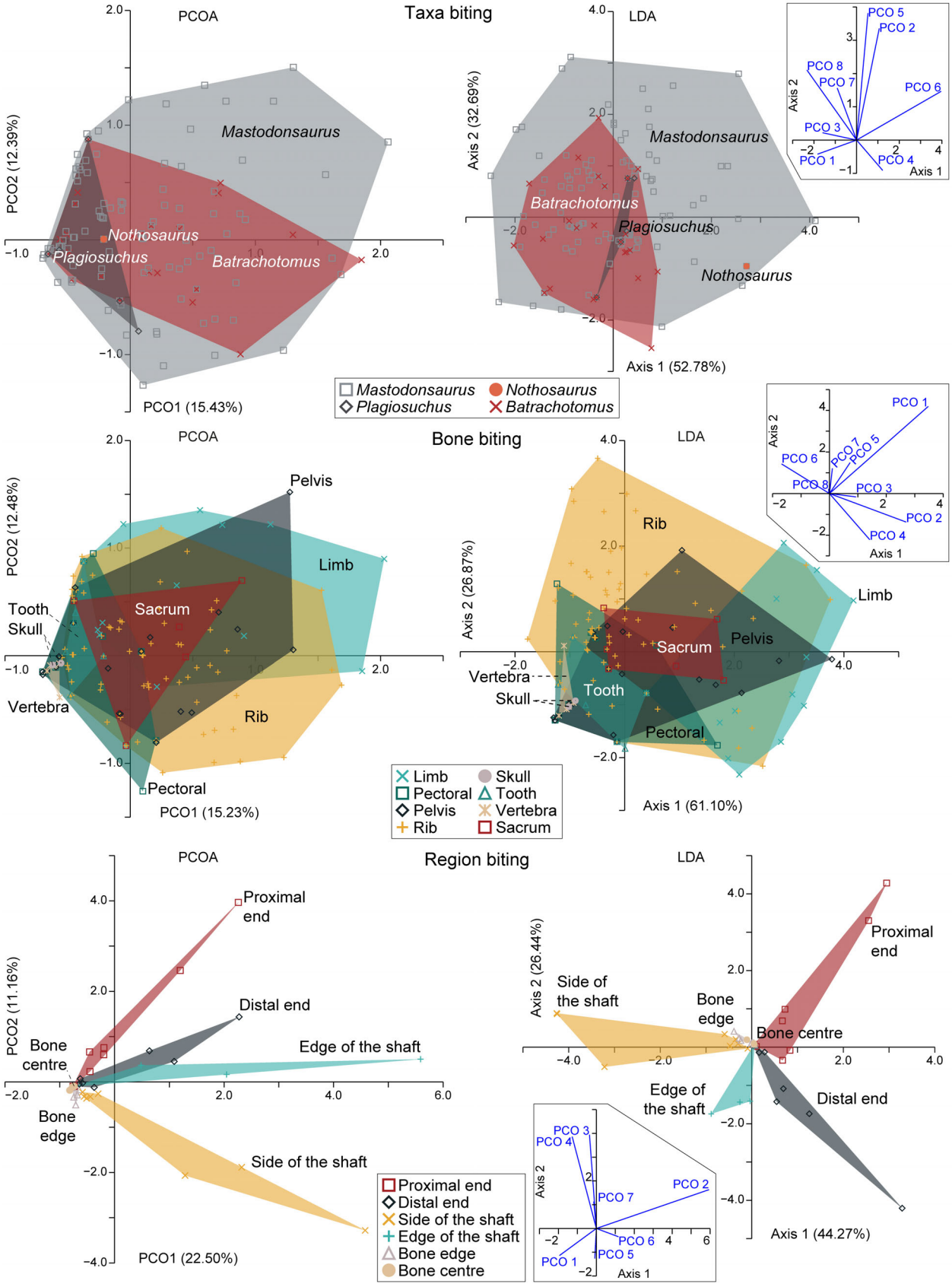
Taxa biting
PCOA
PCO2 (12.39%)
PCO1 (15.43%)
Mastodonsaurus
Nothosaurus
Plagiosuchus
Batrachotomus
LDA
Axis 2 (32.69%)
Axis 1 (52.78%)
PCO 5
PCO 2
PCO 8
PCO 7
PCO 6
PCO 3
PCO 1
PCO 4
Axis 2
Axis 1
Mastodonsaurus
Nothosaurus
Plagiosuchus
Batrachotomus
Bone biting
PCOA
PCO2 (12.48%)
PCO1 (15.23%)
Pelvis
Limb
Sacrum
Tooth
Skull
Vertebra
Rib
Pectoral
LDA
Axis 2 (26.87%)
Axis 1 (61.10%)
PCO 1
PCO 6
PCO 7
PCO 5
PCO 8
PCO 3
PCO 2
PCO 4
Axis 2
Axis 1
Limb
Skull
Pectoral
Tooth
Pelvis
Vertebra
Rib
Sacrum
Region biting
PCOA
PCO2 (11.16%)
PCO1 (22.50%)
Proximal end
Distal end
Bone centre
Edge of the shaft
Bone edge
Side of the shaft
LDA
Axis 2 (26.44%)
Axis 1 (44.27%)
Proximal end
Side of the shaft
Bone edge
Bone centre
Edge of the shaft
Distal end
PCO 3
PCO 4
PCO 7
PCO 2
PCO 6
PCO 5
PCO 1
Axis 2
Axis 1
Proximal end
Distal end
Side of the shaft
Edge of the shaft
Bone edge
Bone centre

FIG. 7. PCOA and LDA results from the bite traces. Biting spaces are compared for each bitten taxon (top), each skeletal region (limbs, pectoral girdle, pelvic girdle, ribs, sacrum, vertebrae, teeth and skull) (middle), and each bone region (proximal and distal ends, side and edge of the shaft, bone edge, and bone centre) (bottom) for the first two ordinates. Percentage of total variation for each ordinate is given in parentheses. Biplots visualizing the factor loadings of the LDA are shown next to the corresponding plot.

one oblique to nearly perpendicular *Knethichnus* between them, outlining an N- or Z-shaped composite trace (Figs 2B, 3E, 5A, C, P). Occasionally, this association is the opposite, with *Linichnus* in-between *Knethichnus* traces (Fig. 5D, S).

Nihilichnus is most commonly associated with *Linichnus* (Data S1), although there are also *Nihilichnus*–*Knethichnus* associations (e.g. Fig. 5B, P, Q, S, T); in both cases, there is usually a relatively sharp transition between both trace morphotypes, though clearly produced by the same tooth. A peculiar association, found in different bones, is that of two gently curved/arched traces of *Knethichnus* outlining a fan or an open triangle (e.g. SMNS 81109, 97012); in some cases (e.g. SMNS 81210) this association consists of a *Knethichnus* trace in each outer end that changes to *Linichnus* in the middle of the composite trace, where the two traces join, or eventually the tooth only generates *Linichnus* (SMNS 80923) (Figs 2H, 5K, I, L; see below). Some (usually long) *Knethichnus* traces show sharp changes in orientation of the grooves (although direction of the grooves changes a few degrees), occasionally with a *Linichnus* and/or *Nihilichnus* trace in between (Fig. 5D, S), resembling the pivoting traces produced by crocodylians (Njau & Gilbert 2016).

Both *Brutalichnus* morphotypes are very commonly in association with *Nihilichnus*, but in some cases they are also in transition from *Knethichnus* and *Linichnus* (Figs 2I, J, 3B, D, 4G, 5T). *Brutalichnus* are mostly found on the end of long bones and bone edges (Figs 3–5; Data S1); when found on shafts, it is usually because the bone was broken from that part, most likely due to the bite that generated the *Brutalichnus* trace (e.g. Fig. 5G).

Several bones also display areas with dense clusters of diverse bite traces, in parallel or in multiple directions, and mostly including *Nihilichnus* and rectilinear to curved *Linichnus* and *Knethichnus* (Figs 2A, K, 3D, E, 5I). Such dense clusters are extremely similar to those produced by crocodylians (Njau & Gilbert 2016; Shale *et al.* 2017), even though their teeth are not ziphodont, unlike those of *Batrachotomus*, the bite maker of the traces analysed herein (see section Identification of the bite maker, below).

Several bones display clusters of (usually abundant) parallel to nearly parallel traces of *Linichnus*, with some associated *Knethichnus* as well, when they build up the aforementioned N- or Z-shaped composite traces (Figs 2B, 3A, E, 5C, D, P). Also, some bones, especially on the edge area of the shafts, preserve two or more traces of *Linichnus* in a V-shape (Figs 2C, D, 5A, E, F, I); sometimes they seem to form a bifurcated trace, corresponding to a single trace with an abrupt change of orientation with respect to the bone, as observed in traces produced by *Varanus komodoensis* (D'Amore & Blumenschine 2009), non-avialan theropods (Jacobsen & Bromley 2009), and crocodylians (Njau & Blumenschine 2006; Njau & Gilbert 2016; Shale *et al.* 2017). In fact, around these V-shaped *Linichnus*, there are usually other coupled traces of *Linichnus*, which are oblique with respect the long axis of the bone and extend in perpendicular directions (Fig. 5I), being somewhat reminiscent of the aforementioned fan-shaped composite trace of *Knethichnus*–(*Linichnus*)–*Knethichnus* (Figs 2H, 5K, L).

Some bones display surfaces completely covered by long traces of *Knethichnus*, with the different traces being roughly oriented in the same direction, and with only slight changes to the angle of the grooves among traces (Fig. 5P). Otherwise, relatively long but thin *Knethichnus* traces (i.e. a few denticles contacted the bone) are also relatively common (Figs 2G–I, 3B, E–F, 5A–B, Q–S). These traces are mostly rectilinear, sometimes with slight, though abrupt, changes of orientation. At the change of orientation point, *Linichnus* and/or *Nihilichnus* may appear (Fig. 5D, S).

On the edge of shafts (but also on some bone ends), deep traces are frequently observed. They are removed flakes of (mostly cortical) bone with *Knethichnus* extending obliquely within the entire pit and *Linichnus* often in one of the short margins of the removed flake (Figs 2D, F, 4G, B, C, E); such traces are likely to be equivalent to the 'periosteal/subcambial bone spalling' of Njau & Gilbert (2016) and the 'flakes' of Drumheller & Brochu (2014). In fact, the outline of these flakes with *Knethichnus* (i.e. a trace resulting from tooth dragging) is very similar to the crocodylian traces resulting from bone spalling (Drumheller & Brochu 2014; Njau & Gilbert 2016; Shale *et al.* 2017).

Several bones also display bite traces on opposing surfaces; these are usually *Nihilichnus* against *Nihilichnus*, but also *Nihilichnus* against *Brutalichnus*, and *Nihilichnus* against *Linichnus* and/or *Knethichnus* (Figs 2A, 3–5). Notably, aligned sets of *Nihilichnus* also occur, outlining an arch (Figs 3D, 4A, H) representing a partial tooth row. These traces are reminiscent of the 'serial bite marks' (in the sense of Binford 1981) generated during a single biting event with multiple teeth impacting on the

TABLE 2. Results of the PERMANOVA and LDA of bite traces.

		Taxon	Bone type	Bone region
PERMANOVA	Total sum of squares	373.800	371.500	413.900
	Within-group sum of squares	367.400	332.800	345.600
	F-value	1.052	2.894	1.658
	p-value	0.373	**0.000**	**0.000**
LDA	Error	0.668	0.560	0.438
	$Error_{Resample}$	0.750	0.654	0.542
	$Error_{Random}$	0.750	0.875	0.833

The spatial overlap of biting spaces between taxa, types of bones and bone regions is indicated (see also Tables S1–S9). **Bold** *p*-values of the PERMANOVA indicate significant differences between biting spaces. LDA results are shown as errors in comparison to random sampling.

bone. Occasionally, such aligned traces are parallel grooves (i.e. *Linichnus*; Fig. 4J–K) indicating that the tooth row moved along the bone, and thus with teeth moving parallel to one another in a single bite.

Machichnus-like traces (Figs 2K, 6D–F) are the only ones not associated with any other biting ichnotaxon. Instead, they are only associated with (abundant) traces of the same morphotype. They are found as clusters of bite traces, being somewhat aligned with the long axis of each trace perpendicular to the major axis of the whole cluster. Therefore, they represent single bites or multiple, repeated strokes, or most likely both.

Distribution of bite traces along the Lower Keuper bones

As aforementioned, bite traces have been identified in five different tetrapod taxa. With the exception of a rib probably corresponding to a chroniosuchid reptile (Fig. 2H), all bones that were anatomically identified were included in the statistical analyses. Statistically, *Mastodonsaurus* bones show the largest anatomical distribution of bite trace types in PCOA 'biting space', followed by *Batrachotomus* and *Plagiosuchus*. All taxon-specific biting spaces show strong overlap (see LDA and PERMANOVA results: Fig. 7; Table 2; Tables S1–S3). The same associations or composite bite traces are found in different bone types and bone regions (Figs 3–5), suggesting that the bones were bitten in similar ways independently from their shape and body region (Figs 7, 8). With the exception of the limbs and vertebrae, taxa show a similar distribution of bite traces across anatomical regions, and the location and identity of the bite traces on individual bones depend on the skeletal region (Figs 7, 8). Thus, all bitten taxa were similarly processed by the bite maker.

The distribution of bite traces along each type of bone (limb, rib, pectoral girdle, sacrum, pelvis, vertebral column, skull and teeth) and bone region (for elongated bones, proximal and distal end, and side and edge of the shaft; for all other bones, bone edge and bone centre) shows remarkable differences (Figs 7, 8; Table 2; Tables S4–S9). The results of the PCOA and LDA (Error: 56%; Error-JK: 65.4%) indicate that bite trace patterns on bones from different body regions strongly overlap with each other, except for the limb bones. The PERMANOVA results ($F = 2.894$; $p < 0.001$) indicate no significant overlap of limbs and vertebrae with other bone regions. Nevertheless, the results show that bones from most body regions were processed by the bite maker in a similar way, as all ichnotaxona are observed on each bone type, skeletal region, and bone region of both *Mastodonsaurus* and *Batrachotomus* (Fig. 8). Each bone region shows a strong overlap in the biting space along PCO1 (Fig. 7). On the other hand, proximal ends, distal ends, side of shafts and edge of shafts of long bones are clearly separated from each other along PCO2. The PERMANOVA analysis also indicates a common biting pattern in different bone regions, which is also evidenced by the presence of equivalent composite bite traces in different bones and bone regions (see Associations of bite traces from the Lower Keuper, above; Figs 3–5; Data S1). Only the bone edge and bone centre were found to be significantly different from the other regions (Fig. 7), although this may result from the different shape of the corresponding bones (those that are non-elongated, such as vertebrae and *Mastodonsaurus* ischia and scapulacoracoids). However, in the LDA (Error: 43.75%; Error-JK: 54.17%) bone ends and shafts are well separated from each other along axis 1. Furthermore, proximal and distal ends as well as sides and edges of shafts are well separated along axis 2. Both the bone edge and centre regions cluster close to the point of origin (Fig. 7).

All in all, the results indicate that different bone regions seem to be more specifically processed by the bite maker when compared with the skeletal regions, but still show common patterns of bite traces. Such differential distribution of bite traces is also observed in the occurrence of each ichnotaxon on each bone type, skeletal region and bone region of *Mastodonsaurus* and *Batrachotomus*, which encompass the bulk of bones with bite traces, most of which are ribs (Fig. 8; Data S1). Note that these counts are based on presence/absence, not the absolute number of each ichnotaxon (i.e. a given ichnotaxon on a bone region is counted as one regardless of whether there is a single or several traces of this same ichnotaxon). In *Mastodonsaurus*, *Nihilichnus* (punctures produced by tooth tips) are markedly more abundant

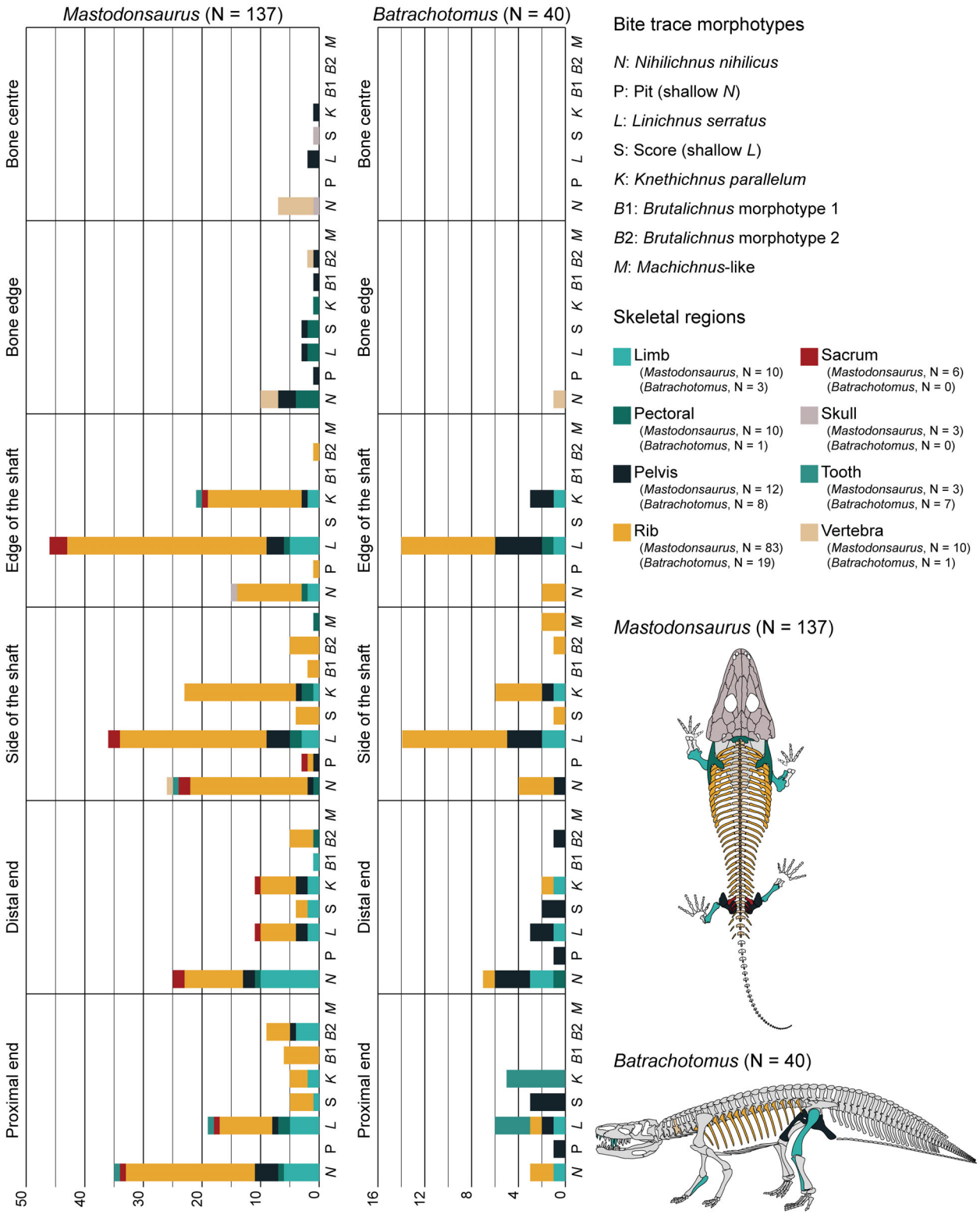

FIG. 8. Counts of bite traces on each bone type and bone region for *Mastodonsaurus* and *Batrachotomus*. Counts are based on single presence; multiple traces of the same morphotype in a bone region are only counted as one, indicating the presence of the given bite trace morphotype. Bones of the restored skeletons are coloured according to the bars of bite traces counts, and as in the bone biting space (skeletal region) of Figure 7. Unknown bones are excluded.

based on count data than the other ichnotaxa on both proximal and distal bone ends, whereas in *Batrachotomus* this only occurs on the distal end (Fig. 8). Long bone ends frequently show traces (mostly *Nihilichnus*, though *Brutalichnus* presence is also notable) on both sides, resulting from a single bite using teeth from the lower and upper jaws (Figs 2A, 3A, C–E; Data S1). The side (the widest) and edge (the narrowest) areas of the shaft show similar distributions on long bones of both *Mastodonsaurus* and *Batrachotomus* (Fig. 8). On shafts, *Linichnus* dominates, followed by *Knethichnus* (which is often associated with the former); notably, the N- or Z-shaped traces, V-shaped traces, and the deep flakes covered with *Knethichnus* are often on the edge of the shaft (Figs 2C–D, F, 3B, E, 4A–C, E, 5C–E, P). Also, in several shafts, *Linichnus* traces are perpendicular (with respect to the bone axis) on the edge area and continue in oblique orientation to the side area. *Nihilichnus* is also relatively common on shafts, especially on ribs of *Mastodonsaurus* (Fig. 8); in fact, the uncinate processes of *Mastodonsaurus* ribs often show *Nihilichnus* traces, which occasionally are in transition to *Linichnus* and/or *Knethichnus* (Fig. 5A, G, H; Data S1). Both morphotypes of *Brutalichnus* are more commonly found on the ends of long bones and bone edges, which is consistent with the destructive nature of the trace. *Nihilichnus* is the dominant ichnotaxon on non-elongated bones (flat or polygonal elements and vertebrae).

Identification of the bite maker

Since most of the observed ichnotaxa are associated and build up regular composite traces with similar distribution in different bones (Figs 2A–J, 3–5, 8; Data S1), it is evident that they were produced by a single taxon. Within the diverse tooth assemblage from the Lower Keuper (Schoch *et al*. 2018), only the ziphodont teeth with laterally compressed, blade-like crowns of the pseudosuchian archosaur *Batrachotomus kupferzellensis* (Gower 1999; Schoch & Seegis 2016; Schoch *et al*. 2018) match most of the surveyed bite traces. Much more restrictive for the identification of the bite maker is the (relatively high) occurrence of *Knethichnus parallelum*, a trace produced by the dragging of denticles on the bone surface, and therefore exclusively produced by ziphodont teeth (Jacobsen & Bromley 2009; D'Amore & Blumenschine 2009, 2012; Pirrone *et al*. 2014). The number of grooves in a given distance and their spacing in each *Knethichnus* trace show the minimum size and spacing of the tracing tooth denticles (D'Amore & Blumenschine 2012). All the analysed *Knethichnus* specimens show a maximum density of 3.5 to 5 grooves/mm, falling in the range of *Batrachotomus* teeth (Gower 1999; Schoch & Seegis 2016; Schoch *et al*. 2018), with a density of 2.8–5.4 denticles/mm on the mesial and 3–4.8 denticles/mm on the distal carina (Data S2). In fact, in the Lower Keuper tetrapod assemblage there are no other known taxa with the same denticle size and density (Schoch *et al*. 2018). Considering the association of *Knethichnus* with the other ichnotaxa (see Distribution of bite traces along the Lower Keuper bones, above), the attribution of most of the identified bite traces to *Batrachotomus* is therefore unambiguous (Data S1). In addition, the deep *Nihilichnus* traces found on some bones (e.g. Fig. 2A) display a rhomboid outline fitting with the teeth of *Batrachotomus*. Similarly, *Nihilichnus* traces corresponding to bisected pits (e.g. Fig. 5M) fit with *Batrachotomus* teeth, as occurs in similar bite traces attributed to phytosaurs (Drymala *et al*. 2021). Furthermore, the distance between aligned traces outlining (partial) tooth rows (e.g. Figs 3D, 4A, H, J–K) fits with the distance between the teeth of *Batrachotomus* jaws. Particularly, the four *Nihilichnus* traces on a *Mastodonsaurus* ischium (SMNS 84244; Fig. 4H) draw a semicircular line that fits with the outline of the premaxillae of a medium-sized *Batrachotomus* (e.g. Gower 1999); each bite trace corresponds to a tooth present in the premaxillae, which would be four (two in each side) according to the alternating replacement of teeth (i.e. the first and third teeth in one premaxilla, and the second and the fourth in the other) as documented by Gower (1999) and observed in the paired premaxillae of SMNS 80260 (Data S2).

The only bite traces most likely not to have been produced by *Batrachotomus* are: (1) small *Nihilichnus* traces on a *Mastodonsaurus* tusk (SMNS 91634) that are aligned and outline a curved arch with little spacing between them (Data S1); (2) the traces found on the ventral surface of two palates (SMNS 80704, 81310) and one mandible (SMNS 92128) of *Mastodonsaurus* (Fig. 6A–C); and (3) all the *Machichnus*-like traces (SMNS 81210, 97014, 97013/5) (Figs 2K, 6D–F), because they are not associated with any other morphotype. Traces on the palates and mandible of *Mastodonsaurus* were all likely to have been produced by a conspecific, especially the paired large *Nihilichnus* on the palate SMNS 80704 and the mandible SMNS 92128 (Fig. 6A–B), which fit well with the morphology and position of the paired tusks of *Mastodonsaurus* mandibles (Schoch & Seegis 2016). Considering the small spacing between clusters of *Machichnus*-like traces (probably produced in single bites and/or repeated strokes on the same area), as well as the notable size and morphological differences with the other ichnotaxa, it can be asserted that the *Machichnus*-like traces were produced by a different taxon that could not be identified. In any case, the bite maker was most probably a relatively small-sized diapsid reptile with serrated teeth (possibly an archosauriform; Schoch *et al*. 2018), given the slightly serrated

margins of some grooves in clusters of *Machichnus*-like traces (Fig. 6E). Within the Lower Keuper tooth assemblage, several tooth morphotypes (mostly of archosauriforms) that could fit with such bite traces have been identified, though some have not been associated with any particular taxon yet (Schoch *et al.* 2018). However, although unlikely considering the inferred behaviour for the formation of bite traces, the possibility that these bite traces were produced by a juvenile specimen of *Batrachotomus* cannot be totally excluded.

Morphology and macroscopic wear on Batrachotomus *teeth*

Given the frequency of tooth–bone contact suggested for *Batrachotomus*, we assessed the type and distribution of abrasive macroscopic wear on 82 premaxillary and 232 maxillary and dentary teeth of this pseudosuchian archosaur. In fact, the surveyed tooth macroscopic wear (including wear, notches, spalling and breakage; Table 1; Fig. 9; Data S2) shows patterns that closely fit with the morphology, associations and distribution of bite traces, as further shown in the Discussion, below. Teeth from Kupferzell (N = 258) and Vellberg-Eschenau (N = 56) show similar macrowear patterns, suggesting no ecological differences between the two localities despite (slight) sedimentological differences (Urlichs 1982; Schoch & Seegis 2016; DS, EM, RRS, pers. obs.) (Fig. 1B).

Box-plots and counts of macrowear show slight but statistically significant differentiation of the macroscopic wear from premaxillary and non-premaxillary teeth (Figs 10, 11), which indicate different usages of each tooth type (see Usage of teeth: correlating tooth wear and bite traces, below). Premaxillary teeth display relatively more wear on the tips than on the carinae, also accounting for a higher degree of abrasion than the non-premaxillary teeth. Wear generally decreases from the tip to the base of both premaxillary and non-premaxillary teeth (e.g. Fig. 9C, D). The tips of premaxillary teeth possess more frequently severe (extreme) wear than those of maxillae and dentaries. Wear on non-premaxillary teeth is more common and severe on the mesial carina than on the distal carina, whereas premaxillary teeth show relatively homogeneous wear over both carinae, though the basal mesial carina (where denticles are often lacking) is significantly less worn than the other regions. Notches show much more differentiation in distribution. On premaxillary teeth, notches are more abundant and severe on the middle and basal distal carina, and a very few occur on the basal mesial carina. On non-premaxillary teeth, notches occur more frequently on the mesial carina; nonetheless, the middle distal carina accounts for the highest occurrence of notches, with a marked difference relative to the other regions. Interestingly, the counts of wear and notches are generally proportionally inverse on both premaxillary and non-premaxillary teeth: wear increases from the basal to the apical regions of both carinae, while notches show an opposite trend (with the exceptions mentioned above; Fig. 11).

Breakage and spalling most commonly occur on the tooth tips. Usually, the surfaces of broken tips are smoothed or polished due to abrasive wear (Fig. 9A–C, G–I), indicating that breakage occurred during the tooth lifetime and thus was most likely to have happened during feeding. Interestingly, premaxillary teeth often show higher degrees of spalling (running from the tip) on the labial than on the lingual side (Data S2), thus indicating that such damage did not result from tooth–tooth contact. Some teeth display severe breakage, with the entire carina completely broken, starting from the tip. Notably, in some cases, only the tip and the apical distal carina display breakage, with a sudden stop of the damage on the carina (Fig. 9E–F).

Microanatomy of Batrachotomus *teeth*

Longitudinal thin sections along the carina reveal that denticles in *Batrachotomus* consist of both enamel and dentine, and thus are ziphodont following the definition of Brink *et al.* (2015) (see also Wang *et al.* 2015; Whitney *et al.* 2020). The tooth crown consists of enamel and bulk dentine, separated by a zone of globular mantle dentine (Fig. 9N–T). Enamel is thickest on the surface of the denticles (*c.* 80 μm), but also towards the mesial and distal carinae (up to 60 μm) (Fig. 9N, Q–S). Enamel thickness also decreases on both the carinae and the sides of the tooth in an apicobasal direction. The enamel of each denticle is separated from that of the adjacent denticle by a channel continuous with the interdental fold (Fig. 9N–O) (Brink *et al.* 2015). Within a denticle, enamel thickness thins toward the interdental fold (Fig. 9N, Q, R). Enamel spindles are rare overall, but occasionally present in the denticles (Fig. 9P). Dentine tubules originating within the fold curve pulpward towards the base of the denticle, becoming more densely distributed between folds (as with plicidentine). The base of the interdental fold consists of globular dentine, but globular mantle dentine is thin to absent in the denticles themselves (Fig. 9N–P, T). Sclerotic dentine was difficult to recognize: there are fewer dentine tubules surrounding the interdental fold, and this region appears to mineralize more heavily between the least worn and a heavily worn tooth. However, wear on individual denticles (Fig. 9Q, R) does not appear to influence the development of sclerotic dentine, nor does sclerotic dentine develop on the tips of denticles worn down to the bulk dentine.

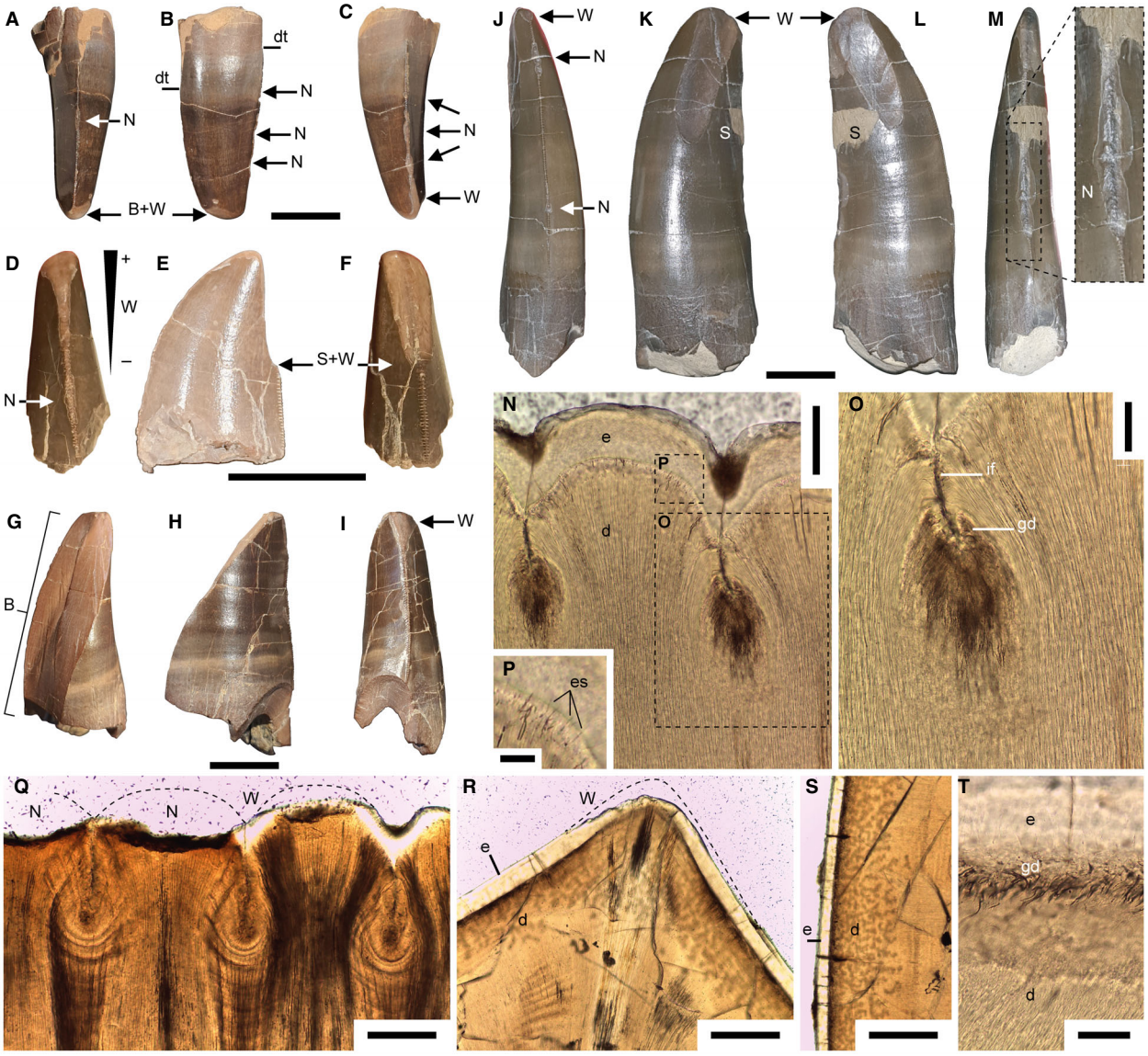

FIG. 9. Macroscopic wear and microanatomy of *Batrachotomus* teeth. A–C, left premaxillary tooth SMNS 97009/4. D–M, non-premaxillary teeth: SMNS 97009/5 (D–F), 97009/3 (G–I), and 97009/2 (J–M). Images show medial (A, D, G, J), labial (B, K), lingual (E, H, L), and distal (C, F, I, M) views. N–P, longitudinal thin section of denticles from the apical distal carina of the non-premaxillary tooth SMNS 97009/16 in transmitted light. Q, worn denticles from the middle mesial carina of SMNS 97009/8 in longitudinal section. R–S, transverse section of SMNS 97009/17, showing thicker enamel close to the carina (also showing a worn denticle) (R) compared to the lateral portion (S). T, detail of the dentine–enamel junction of SMNS 97009/16. Dashed lines in Q and R indicate the supposed original (unworn) denticle shape. *Abbreviations*: B, breakage; d, dentine; dt, end point of denticles; e, enamel; es, enamel spindles; gd, globular dentine; if, interdental fold; N, notch; S, spalling; W, wear. Scale bars represent: 10 mm (A–C; D–F; G–I; J–M); 100 µm (N, Q); 40 µm (O, T); 25 µm (P); 200 µm (R–S).

Comparison of Batrachotomus *teeth with those of theropod dinosaurs and other archosauromorphs*

According to our LDA analysis of dental measurements in different archosauromorphs, including non-avialan theropods (see Hendrickx *et al.* 2015; Hoffman *et al.* 2019), the teeth of *Batrachotomus* plot in between the area of non-spinosaurid Megalosauroidea and Spinosauridae, and are further surrounded by the tooth morphospaces of Allosauroidea, Ceratosauria, Tyrannosauroidea and Archosauromorpha morphotype A (Fig. 12). All these taxa represent apex predators with ziphodont teeth. If Spinosauridae are treated as an independent group, the LDA (Error: 43.05%; $\text{Error}_{\text{Resample}}$: 46.03%) identifies 19 out of 23 *Batrachotomus*

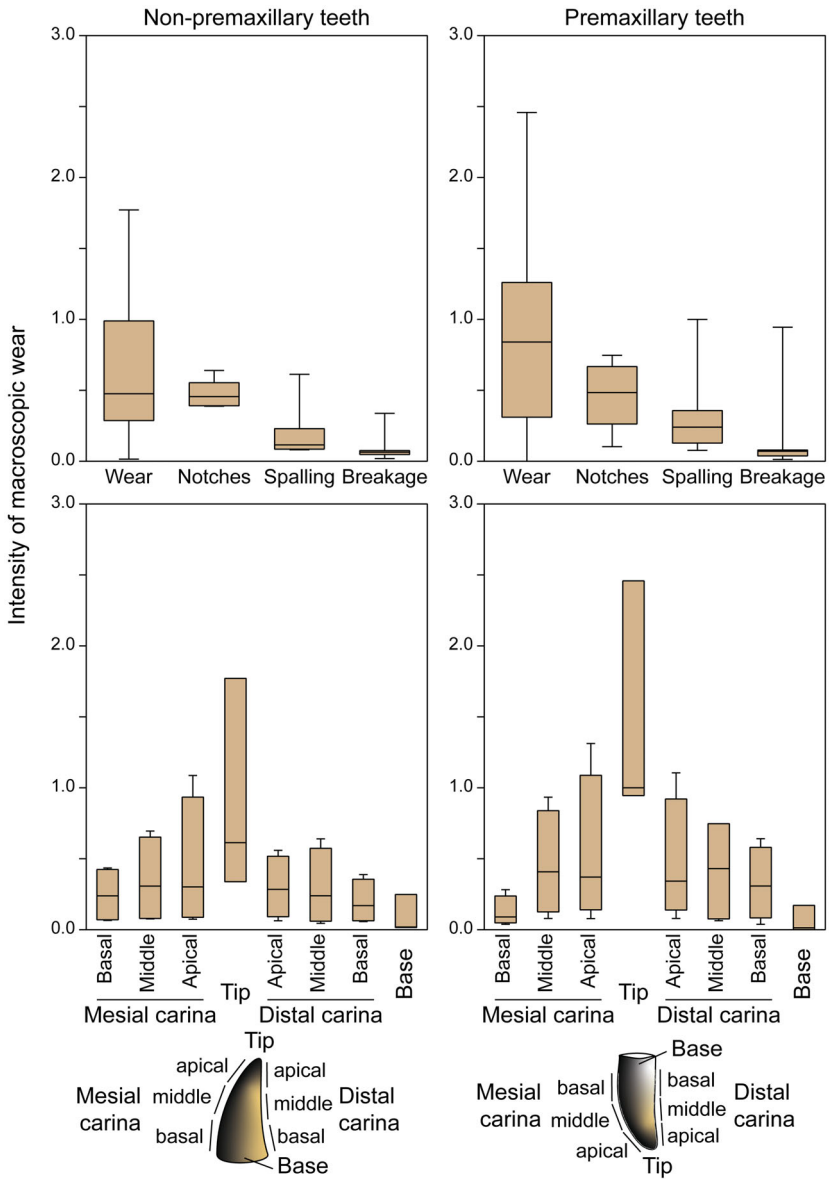

FIG. 10. Box-plots of wear intensity on *Batrachotomus* teeth (1 = low; 2 = high; 3 = extreme). Above, intensity of the different types of macrowear. Below, intensity of macroscopic wear (including all four types) for each portion of the carinae, tip, and base of the crown.

teeth correctly (Table 3). One tooth is identified as Coelophysoidea and three as non-spinosaurid Megalosauroidea. Treating *Batrachotomus* teeth as unknown, they are most commonly identified as Allosauroidea (five times), Archosauromorpha morphotype A (six times) and Spinosauridae (five times). The PERMANOVA indicates an overlap of the *Batrachotomus* tooth morphospace with that of Archosauromorpha morphotype A, Ceratosauria, Erpetosuchidae, 'Rauisuchia' and Suchia.

When Spinosauridae are grouped together with the other Megalosauroidea, LDA (Error: 42.38%) classifies 14 teeth correctly, while the other teeth are identified either as Allosauroidea, Ceratosauria, Dromaeosauridae, Megalosauroidea or Tyrannosauroidea. After cross-validation of the LDA ($Error_{Resample}$: 45.14%), only 12 *Batrachotomus* teeth are correctly identified, while nine teeth are found to belong to Megalosauroidea (Table 3). Treating *Batrachotomus* teeth as unknown, they are identified 16 times as Megalosauroidea (Table 3). Based on this grouping, the PERMANOVA found additional overlap with the morphospaces of Megalosauroidea and Silesauridae.

DISCUSSION

Usage of Batrachotomus *teeth: correlating tooth wear and bite traces*

Associated and composite bite traces, combined with a differential distribution of each bite trace morphotype in each skeletal and bone region (Fig. 8; Data S1) and

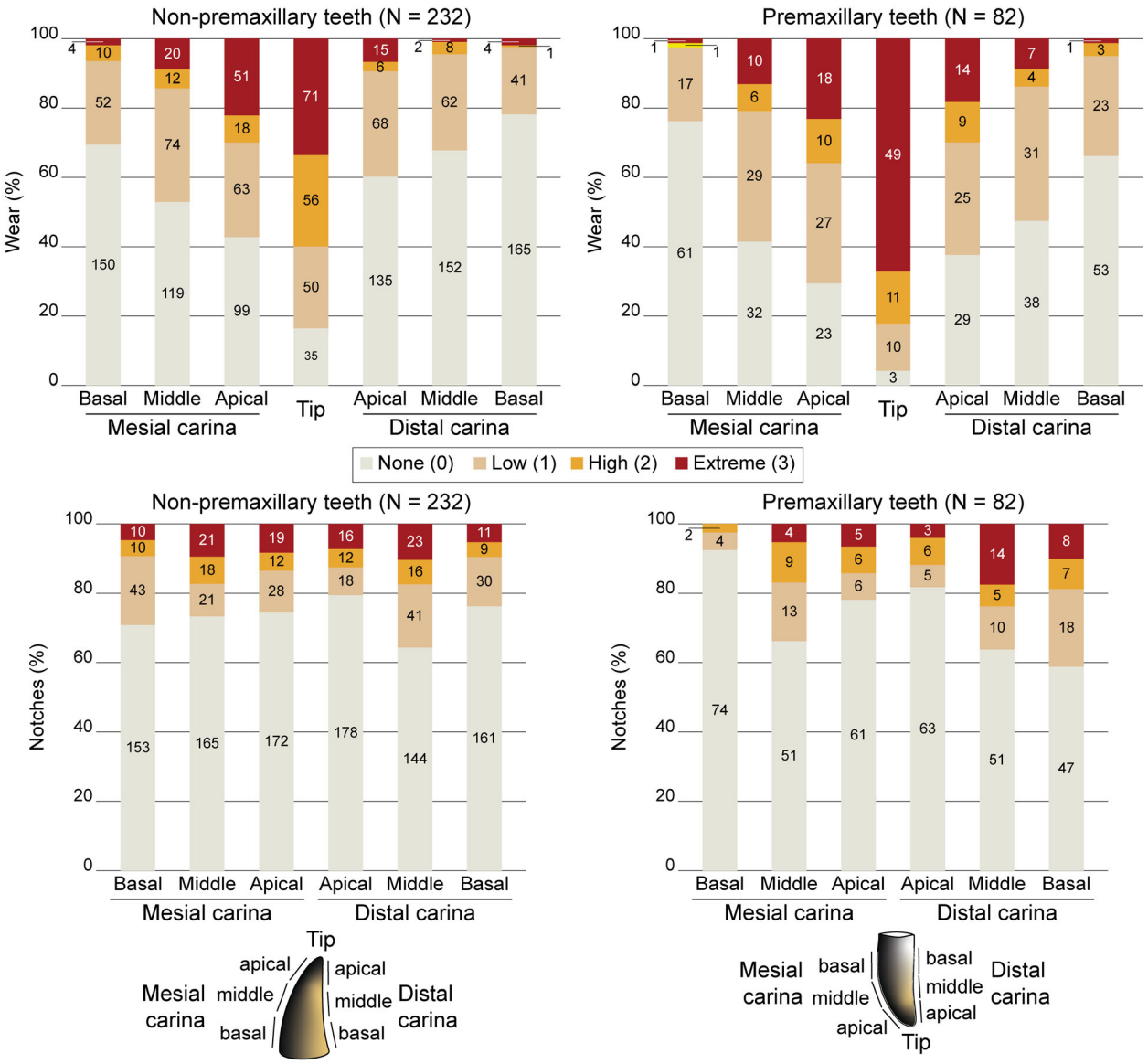

FIG. 11. Percentage of abrasion (wear and notches) on *Batrachotomus* teeth. The degree of abrasion (none, low, high, extreme) is accounted. Numbers within colour bars represent counts (absolute occurrences) of each degree of abrasion in each tooth portion. Unknown values ('?' in Data S2) are excluded, thus the sum of values of each bar is lower than the total number of teeth (N) analysed.

the macroscopic wear on *Batrachotomus* teeth, allow the movement of teeth on bones, and thus the most probable behaviours and usages of the carcasses, to be reconstructed.

As shown in 'Morphology and macroscopic wear on *Batrachotomus* teeth' above, tooth tips, especially from the premaxilla, showed the most wear (Figs 10, 11), correlating with the dominance of *Nihilichnus* traces, especially on the ends of ribs and limb bones (Fig. 8), and also on the uncinate processes of *Mastodonsaurus* ribs (Fig. 5A, G, H). Such puncture traces are often aligned and found on opposing bone surfaces, outlining the tooth rows (Figs 3D–E, 4H). These features indicate a potential dismemberment of the carcasses in order to reach fleshy and nutrient-dense regions, as done by extinct and extant crocodylians (Njau & Blumenschine 2006; Njau & Gilbert 2016). Dismemberment and defleshing strokes would have been violent in some cases, as the *Brutalichnus* traces and the relatively high amount of breakage of tooth tips and carinae suggest. *Brutalichnus* is often associated with *Nihilichnus*, but also with *Knethichnus* and *Linichnus* (Figs 2–5; Data S1), indicating that there were pullbacks

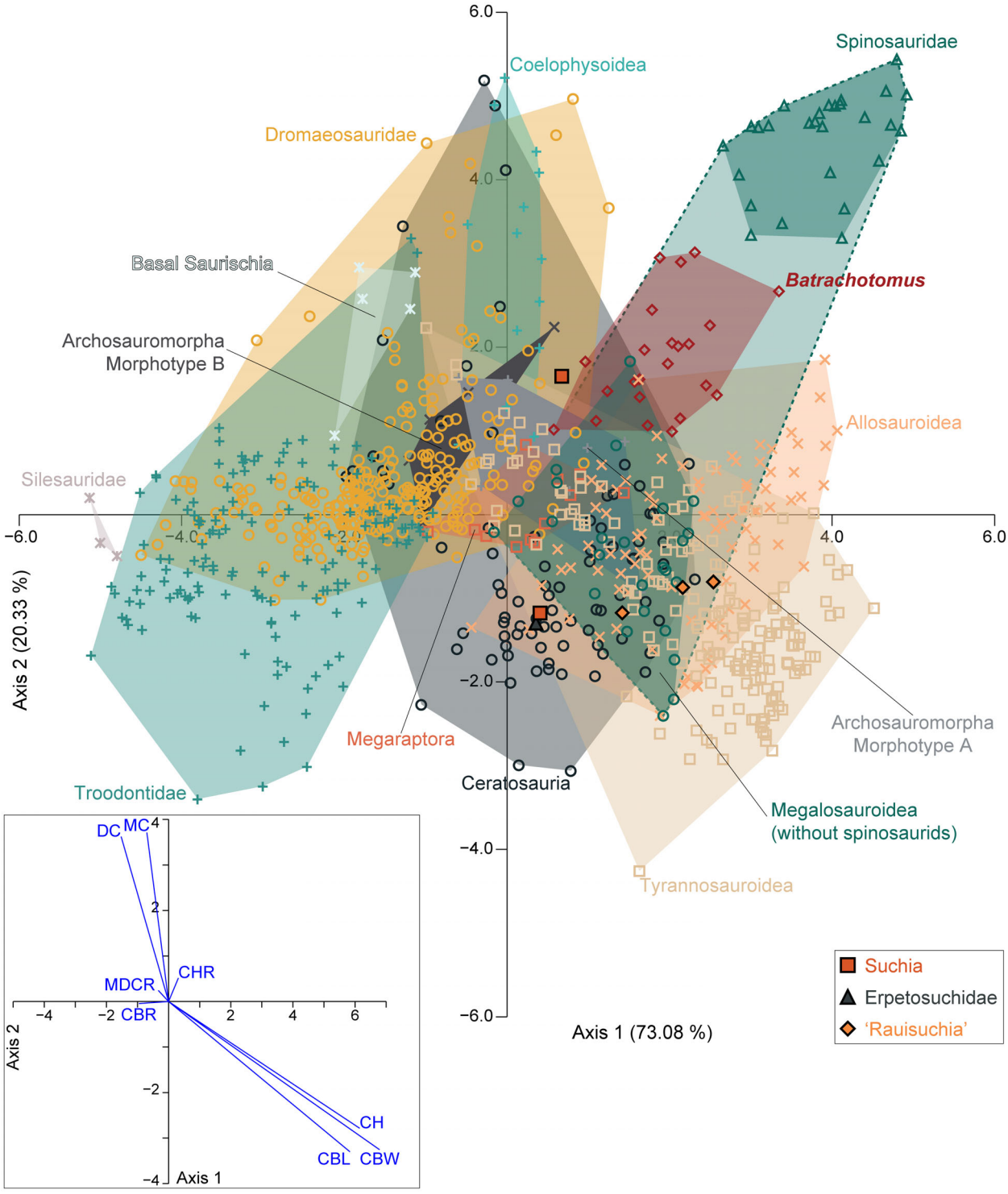

FIG. 12. LDA results of archosauromorph teeth. Plot comparing teeth measurements of *Batrachotomus* with that of different archosauromorphs, including various non-avialan theropod dinosaur groups. Spinosaurids are separated from Megalosauroidea; the dashed line shows the whole area occupied by megalosauroids, mostly overlapping that of *Batrachotomus*. Percentage of total variation for each ordinate is given in parentheses. The factor loadings of the LDA are visualized as a biplot.

TABLE 3. Results of the PERMANOVA and LDA of tooth measurements.

Group	All Megalosauroidea				Spinosauridae separated			
	PERMANOVA		LDA		PERMANOVA		LDA	
	F-value	*p*-value	Classification	Unknown	*F*-value	*p*-value	Classification	Unknown
Batrachotomus	NA	NA	14 (12)	NA	NA	NA	19 (19)	NA
Allosauroidea	42.430	0.012	3 (0)	2	42.430	0.014	0 (0)	5
Archosauromorpha morph. A	7.425	**0.096**	0 (0)	2	7.425	**0.095**	0 (0)	6
Archosauromorpha morph. B	22.410	0.024	0 (0)	0	22.410	0.027	0 (0)	0
Basal Saurischia	71.430	0.012	0 (0)	0	71.430	0.014	0 (0)	0
Ceratosauria	6.244	**0.588**	2 (0)	0	6.244	**0.843**	0 (0)	0
Coelophysoidea	82.920	0.012	0 (0)	0	82.920	0.014	1 (1)	2
Dromaeosauridae	123.100	0.012	1 (0)	0	123.100	0.014	0 (0)	0
Erpetosuchidae	2.271	**1.000**	0 (0)	0	2.271	**1.000**	0 (0)	0
Megalosauroidea	3.626	**1.000**	2 (9)	16	15.340	0.014	3 (3)	3
Megaraptora	16.090	0.024	0 (1)	1	16.090	0.014	0 (0)	0
Rauisuchia	11.910	**0.072**	0 (0)	0	11.910	**0.054**	0 (0)	0
Silesauridae	171.400	**0.072**	0 (0)	0	171.400	0.041	0 (0)	0
Spinosauridae	NA	NA	NA	NA	28.590	0.014	0 (0)	5
Suchia	2.495	**1.000**	0 (1)	2	2.495	**1.000**	0 (0)	2
Troodontidae	128.300	0.012	0 (0)	0	128.300	0.014	0 (0)	0
Tyrannosauroidea	35.390	0.012	1 (0)	0	35.390	0.014	0 (0)	0

The spatial overlap between *Batrachotomus* and other archosauromorph teeth (including various non-avialan theropod dinosaurs) is indicated. On the left, Spinosauridae are included within Megalosauroidea; on the right they are separated. In each case, *Batrachotomus* teeth were treated as 'classified' and 'unknown' for the LDA. **Bold** *p*-values of the PERMANOVA analysis indicate a significant degree of overlap between *Batrachotomus* and other archosauromorphs. Numbers in parentheses in the LDA sections show number of classifications after resampling. NA, not applicable.

and/or repeated strokes associated with these more destructive bites.

The amount and distribution of wear and notches along the tooth carinae are consistent with the generation of most *Linichnus*, *Knethichnus*, and their associations (N/Z-, fan- and V-shaped composite traces, and clusters of *Linichnus*; Figs 2–5). Tooth crowns contacted bones in repeated strokes to deflesh and tear carcasses, leaving composite traces similar to those of crocodylians (Njau & Blumenschine 2006; Njau & Gilbert 2016), occasionally misinterpreted as bone modifications by hominids (Shale *et al.* 2017). Nonetheless, each individual bite trace is more similar to those of non-avialan theropods and *V. komodoensis* (D'Amore & Blumenschine 2009; Jacobsen & Bromley 2009), in other words, taxa with ziphodont teeth. Higher amounts of abrasion in the apical and middle mesial carina, especially of non-premaxillary teeth, are consistent with this interpretation of repeated strokes (Fig. 11). The mesial carina would have more easily reached the bone and also had a wider range of motion than the distal carina (D'Amore & Blumenschine 2009). Similarly, the parallel and oblique orientations of *Knethichnus* with respect to the bone long axes (Data S1) indicate lateral movement of tooth crowns. In contrast, the common (short) bite traces on the edge of the shafts were likely to have been produced by the distal carinae. A pullback when tearing and dismembering carcasses with the distal carina wedged into the bone surface (D'Amore & Blumenschine 2009; Njau & Gilbert 2016) would have generated both *Knethichnus* within relatively deep flakes or hacks (Figs 2F, 3B, 4A–C; see also Jacobsen & Bromley 2009, fig. 3B) and *Linichnus*, with tooth crowns perpendicular and oblique to the bone long axes, and resulted in the observed markedly higher number of notches on the distal carinae of premaxillary teeth and the middle distal carinae of non-premaxillary teeth (Fig. 11). The usual lack of denticles on the basal portion of the mesial carina of premaxillary teeth (Fig. 9B; Data S2) probably responds to a low functionality of this region (D'Amore 2009), which is much less worn than the rest of the crown (Figs 10, 11). Thus, the observed pattern of macroscopic wear in the teeth of *Batrachotomus* provides complementary support for its identity as the bite maker.

In some fossil taxa, tooth–tooth contact (attritional wear) has been invoked to explain patterns of carinal wear and basal facets (Schubert & Ungar 2005; Young

et al. 2012). We consider such explanations unlikely in *Batrachotomous*. The bite trace assemblage clearly supports extensive carina–bone contact as described above. Spalled teeth usually display damage on both labial and lingual sides (Fig. 9K, L); if such damage was generated due to occlusion, these teeth would have contacted the opposing teeth on both their lingual and labial sides, which is very unlikely or even biomechanically impossible. In fact, when the mouth of *Batrachotomus* was closed (see reconstruction by Gower & Schoch 2009), teeth from the upper jaw remain externally placed, thus only their lingual side could have contacted the labial side of teeth from the lower. Therefore not all spalling (if any) could result from tooth–tooth contact. Similarly, premaxillary teeth are usually more worn towards the labial side (Data S2), the side that would have never occluded with teeth from the mandible.

The role of microanatomy on the usage of Batrachotomus *teeth*

The microanatomy of *Batrachotomus* teeth (Fig. 9N–T) shows adaptations conferring resistance to carinal wear and breakage caused by tooth–bone contact seen in other hypercarnivores engaging in puncture and pull feeding (non-avialan theropod dinosaurs and gorgonopsian synapsids: D'Amore 2009; Brink *et al.* 2015; Wang *et al.* 2015; Whitney *et al.* 2020). The loss of globular mantle dentine at the tips of the denticles, combined with its presence at the enamel–dentine junction elsewhere along the tooth crown, has been interpreted as an adaptation for wear resistance in the denticles; in addition, elasticity elsewhere in the tooth has been inferred to confer resistance to breakage (Brink *et al.* 2015). The deep interdental folds would have helped to dissipate stress forces on the teeth (Brink *et al.* 2015; Gignac & Erickson 2017); globular mantle dentine as found at the bases of the folds has been linked to blocking crack propagation and increasing tissue elasticity (Wang *et al.* 2015). The sudden stop of breakage on the distal carina observed in *Batrachotomus* (Fig. 9E–F; Data S2) is consistent with this functional interpretation of deep interdental folds. Enamel thickness in *Batrachotomus* is quite thin relative to that in both therapsids and *Tyrannosaurus* (Whitney *et al.* 2020), but is within the reported range of 'rauisuchians' and other theropods (Sander 1999; Wang *et al.* 2015). Sander (1999) reported that 'rauisuchian' enamel was thinnest on the tops of the denticles; this is in contrast to what we observed in *Batrachotomus* (Fig. 9R, S), but might be attributable to carinal wear in the tooth sampled by Sander (1999) (see worn denticles in longitudinal and transverse section in Fig. 9Q, R). Here, considering the distribution and types of macrowear, variation in enamel thickness across the tooth crown in *Batrachotomus* is correlated with variation in wear, with enamel thickness greatest in those areas of the tooth most prone to contact with bone during feeding (Fig. 9Q–S). The overall tooth microstructure of *Batrachotomus* has been interpreted as a convergent character of hypercarnivores engaging in puncture and pull feeding (D'Amore 2009; Whitney *et al.* 2020), increasing wear resistance of the denticles and while maintaining overall tooth elasticity (Brink *et al.* 2015; Wang *et al.* 2015; Gignac & Erickson 2017). This functional interpretation is congruent with the wear and breakage patterns of *Batrachotomus* teeth described here (see Morphology and macroscopic wear on *Batrachotomus* teeth, above; Fig. 9; Data S2) indicating specializations for puncture and pull feeding by *Batrachotomus* on various large sympatric vertebrates.

Palaeoecological implications of the feeding habits and taphonomy of Batrachotomus

Feeding ecology and taphonomy. The distribution and frequency of bite traces is suggestive of different behaviours by *Batrachotomus*, including scavenging, cannibalism and predation. We found a strong correlation between the frequency of bone types in a *Mastodonsaurus* skeleton and the frequency with which each bone is bitten (Fig. 13), suggesting a systematic and virtually complete exploitation of carcasses by *Batrachotomus*.

Different bones of *Mastodonsaurus* and *Batrachotomus* from Kupferzell were found in clusters reliably referred to single individuals (Wild 1980; Gower 1999; Schoch 1999; Gower & Schoch 2009; Data S1). These associations, together with the lack of bone sorting, indicate that there was little-to-no transport of carcasses, at least in Kupferzell. In fact, in Vellberg-Eschenau, where bite traces are notably lower in number than in Kupferzell (Data S1), evidence of bone sorting has been reported (Schoch & Seegis 2016). This would indicate a higher washout of carcasses in Vellberg-Eschenau, further noting slight sedimentological differences (Urlichs 1982; DS, EM, RRS, pers. obs.; Fig. 1B). Nonetheless, between Kupferzell and Vellberg-Eschenau there are no differences in the location of bite traces on bones nor in the macroscopic wear of *Batrachotomus* teeth (Data S1, S2). These similarities suggest that, as a whole, this bite trace assemblage is not an unusual scenario under specific environmental conditions, but the record of the usual feeding behaviour of the bite maker. Hypothetically, this is also indicated by the predictable distribution of composite bite traces in different taxa, different bones, and different bone regions (Figs 3–5, 7, 8) suggesting that, during feeding, *Batrachotomus* modified bones in a regular, monotonous manner.

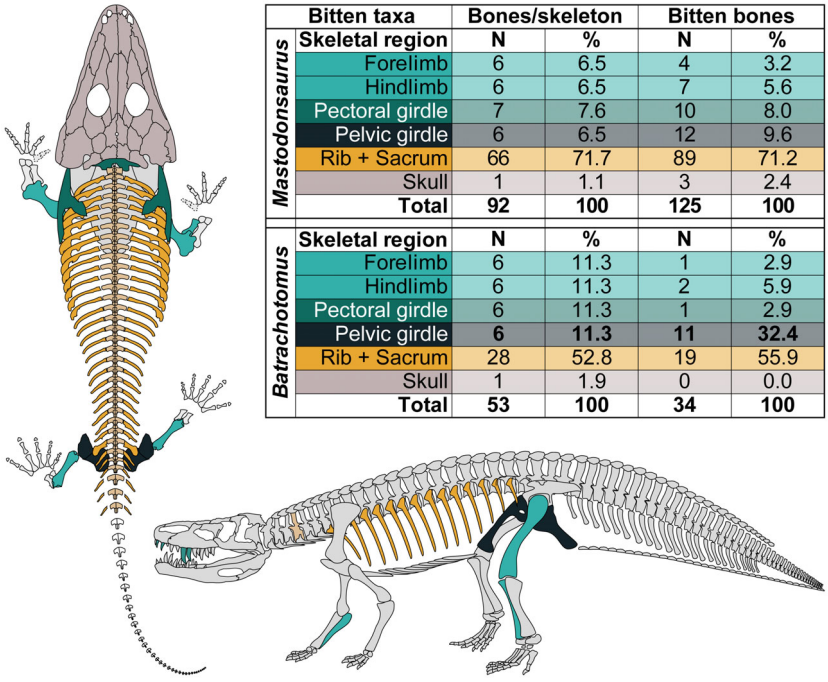

Bitten taxa		Bones/skeleton		Bitten bones	
Mastodonsaurus	**Skeletal region**	**N**	**%**	**N**	**%**
	Forelimb	6	6.5	4	3.2
	Hindlimb	6	6.5	7	5.6
	Pectoral girdle	7	7.6	10	8.0
	Pelvic girdle	6	6.5	12	9.6
	Rib + Sacrum	66	71.7	89	71.2
	Skull	1	1.1	3	2.4
	Total	**92**	**100**	**125**	**100**
Batrachotomus	**Skeletal region**	**N**	**%**	**N**	**%**
	Forelimb	6	11.3	1	2.9
	Hindlimb	6	11.3	2	5.9
	Pectoral girdle	6	11.3	1	2.9
	Pelvic girdle	**6**	**11.3**	**11**	**32.4**
	Rib + Sacrum	28	52.8	19	55.9
	Skull	1	1.9	0	0.0
	Total	**53**	**100**	**34**	**100**

FIG. 13. Frequency of bitten bones of *Mastodonsaurus* and *Batrachotomus*. Numbers of bones (N) account for the bones that are known for each taxon and skeletal region (e.g. forelimb includes six bones: two humeri, two radii and two ulnae); teeth, phalanges, tarsals, carpals and vertebrae are excluded because their total amount per skeleton is unknown. Sacral ribs (differentiated in the statistical analyses) are here counted together with thoracic and caudal ribs. Restored skeletons are coloured according to the skeletal regions shown in the table and in Figures 7 and 8. Note the high percentage of bitten bones from the pelvic girdle of *Batrachotomus*, being nearly three times the percentage of these bones per skeleton (highlighted in bold).

The distribution and frequency of bite traces produced by *Batrachotomus* across bone regions (Fig. 8) is conspicuously similar to that of crocodylians (e.g. Njau & Blumenschine 2006; Drumheller & Brochu 2014, 2016; Njau & Gilbert 2016; Shale *et al.* 2017). As documented in extant crocodylians by Drumheller & Brochu (2014), the bones bitten by *Batrachotomus* display more penetrative bite traces on the ends of long bones (deep *Nihilichnus* and *Brutalichnus*). Njau & Blumenschine (2006) associated the presence of relatively deep traces to disarticulation attempts, which was also likely to have been the case for the bones bitten by *Batrachotomus* (see Usage of Batrachotomus teeth: correlating tooth wear and bite traces, above). Otherwise, also like in crocodylians (Drumheller & Brochu 2014), the shafts of long bones from the Lower Keuper more commonly (though not exclusively) display relatively shallow grooves (*Linichnus* and *Knethichnus*) that usually do not remove the entire bone cortex and are oriented oblique to perpendicular with respect to long bone axis (e.g. Fig. 3D, E; Data S1). Similarly, spalled flakes of bone, often covered with *Knethichnus*, are mainly found on the shaft of long bones (e.g. Figs 2D, F, 3A–C), also reminiscent of those produced by crocodylians (Drumheller & Brochu 2014; Njau & Gilbert 2016). Such bite traces are likely to be associated with defleshing rather than disarticulation, as has been suggested for crocodylians (Njau & Blumenschine 2006). All in all, the differential distribution of bite traces supports the hypothesis of different usage for each bone region, in agreement with the statistical results (Fig. 7) and further pointing to conserved feeding behaviour in pseudosuchians (Fig. 14).The incompleteness of skeletons would suggest habitats roamed by scavengers (Hungerbühler 1998), tearing carcasses and thus facilitating the loss of specific parts that otherwise would have been preserved. Similarly, the high abundance of shed teeth within mudstones also indicates a low energy environment inhabited by several individuals (Hungerbühler 1998; Augustin *et al.* 2020). Further evidence of scavenging is provided by the presence of bite traces produced by much smaller organisms than *Batrachotomus*. The *Machichnus*-like traces suggest abandoned corpses consumed by small-sized scavengers (probably archosauriforms; see teeth in Schoch *et al.* 2018) that could reach carcasses when relatively high nutrient-value regions (such as the rib cage) were still available (Drumheller *et al.* 2020). Therefore, even though there may have been periods of stressed environments (e.g. droughts) as indicated by histological data from *Batrachotomus* bones (Klein *et al.* 2017), scavenging was not an unusual habit.

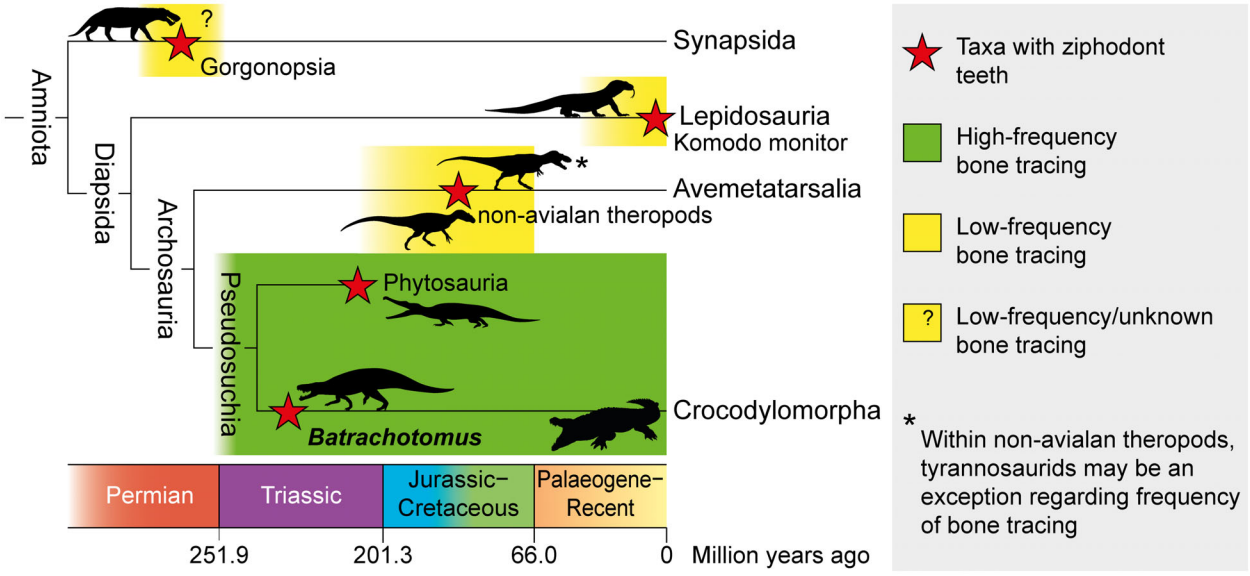

FIG. 14. Simplified phylogeny of amniotes focused on taxa with ziphodont teeth. Age distribution of each clade follows literature cited throughout the manuscript. Potential high-frequency of bone tracing by tyrannosaurids (*) after Hone & Rauhut (2010) (but see discussion in Drumheller *et al.* 2020). Silhouettes from: PhyloPic (http://phylopic.org: Steven Traver (crocodile; CC0 1.0); Scott Harman (non-avialan theropods; CC BY-NC-SA 3.0); Wikimedia Commons, Dmitry Bogdanov (gorgonopsian; CC BY 3.0); *Batrachotomus*, phytosaur and Komodo monitor are author originals.

Remarkably, *Batrachotomus* also fed on conspecifics (Figs 2C–E, G, 3F, 4I–K, 5E, N, 8; Data S1), representing one of the few cases of cannibalism in the archosaur fossil record, previously only reported in non-avialan theropods (Rogers *et al.* 2003; Longrich *et al.* 2010; Drumheller *et al.* 2020), but well-known in present-day crocodylians (Cott 1961). Most of the bite traces on *Batrachotomus* bones are concentrated on ribs and pelvic elements (Fig. 13), which give access to the nutrient-rich viscera and muscles of the tail and hindlimbs. Considering their location on the bones and the lack of evidence of healing, these traces could not have been produced in a living specimen; therefore, they indicate feeding rather than non-trophic intraspecific interactions such as social behaviour. This latter behaviour is known from both fossil pseudosuchians (including crocodylians) (Abel 1922; Buffetaut 1983; Avilla *et al.* 2004; Katsura 2004) and present-day crocodylians (Kälin 1936; Cott 1961; Webb & Manolis 1983), and mostly results in wounds on skull bones (either healed or not) and/or traumatic pathologies on regions of the skeleton that can be reached in a living individual. The *Batrachotomus* teeth preserving *Knethichnus* and *Linichnus* traces on their labial surfaces (Data S1) provide conclusive evidence of intraspecific interaction, possibly competition, among living individuals and are consistent with aggressive interactions seen in fossil pseudosuchians and extant crocodylians (Abel 1922; Cott 1961; Buffetaut 1983). This also agrees with purported evidence for gregariousness in Triassic pseudosuchians (França *et al.* 2011; Nesbitt *et al.* 2013, 2020).

Batrachotomus was less frequently bitten than *Mastodonsaurus* (Fig. 8; Data S1), being a more occasional food source, and possibly representing evidence of scavenging behaviour. Thus, under unstable environmental conditions, *Batrachotomus* possibly adopted cannibalism. Nonetheless, the relatively high number of *Batrachotomus* bones with bite traces suggests that cannibalism was not a totally unusual feeding habit. The frequency of bitten bones with respect to their number in a skeleton of *Batrachotomus* (Fig. 13) suggests that carcasses of this taxon were not completely exploited and, as the *Machichnus*-like traces on *Batrachotomus* ribs suggest, small-sized scavengers did have access to them (Drumheller *et al.* 2020) (see above).

The large *Nihilichnus* found on opposing surfaces of *Mastodonsaurus* femora (Fig. 3C–E), even preserving the outline of the tooth (Fig. 2A), indicate active predation, as they are strikingly similar to those produced by large Triassic predatory archosaurs (Niedźwiedzki *et al.* 2011; Drumheller *et al.* 2014; Qvarnström *et al.* 2019), Cretaceous crocodyliforms (Noto *et al.* 2012; Boyd *et al.* 2013) and Miocene caimans (Pujos & Salas-Gismondi 2020), all resulting from biting the limbs to disable prey during active hunting. This suggests that *Batrachotomus* individuals would have attacked *Mastodonsaurus* on their hindlimbs from the rear, as observed in crocodylians (Cott 1961; Pujos & Salas-Gismondi 2020), to avoid a

potentially dangerous face-to-face encounter. Bones with more destructive bite traces, such as *Brutalichnus* and deep *Nihilichnus*, show fractures with saw-toothed margins (Figs 2I–J, 3C–D, 4G–I 5G, J), indicative of damage to fresh bones (Britt *et al.* 2009). However, healed bite traces indicating attack survival (Drumheller *et al.* 2014) have not been found. Thus, if hunting did occur, all the evidence indicates a predominance of successful attacks. Further interaction between *Mastodonsaurus* and *Batrachotomus* is recorded by two *Mastodonsaurus* tusks showing *Linichnus* and *Knethichnus* traces (Data S1). Since no bite traces on *Mastodonsaurus* skull bones were produced by *Batrachotomus* (Fig. 6A–C), it is unlikely that these bite traces on teeth represent feeding; rather they probably represent a face-to-face interaction.

Considering that *Mastodonsaurus* most commonly roamed (sub-)aquatic habitats (Schoch & Milner 2000; Mujal & Schoch 2020), *Batrachotomus* would potentially also have hunted in such environments. Nonetheless, evidence of desiccation and relatively long-term aerial exposure in the Kupferzell deposits (Wild 1980; Urlichs 1982; RRS, DS, EM, pers. obs.; Fig. 1B) could indicate that *Mastodonsaurus* individuals were trapped in shallow pools where they were hunted by *Batrachotomus*. The ability of *Batrachotomus* to forage in an aquatic habitat is consistent with the dominance of piscivorous tooth types in the Untere Graue Mergel deposits (Schoch *et al.* 2018) and the bite traces of *Batrachotomus* on the bones of the aquatic sauropterygian reptile *Nothosaurus* (Fig. 5R). 'Rauisuchians' (e.g. *Postosuchus*) are usually interpreted as large, terrestrial hypercarnivores (Nesbitt *et al.* 2013); however, the ability of some genera to exploit aquatic food sources has previously been noted (Nesbitt 2011). Furthermore, the strongly convex ventral margin of the maxilla and dorsoventral expansion of the anterior end of the dentary in *Batrachotomus* (Gower 1999) resembles the morphology of large-bodied theropod dinosaurs with ichthyophagous behaviour (Charig & Milner 1997; Marsh & Rowe 2020).

Palaeoecological implications for archosaurs. The aforementioned morphological similitudes between the dentaries of *Batrachotomus* and ichthyophagous theropods are in accordance with the similarities between the teeth of *Batrachotomus* and megalosauroids (see Comparison of Batrachotomus teeth with those of theropod dinosaurs and other archosauromorphs, above; Fig. 12; Table 3), a theropod clade that evolved piscivorous adaptations (Charig & Milner 1997; Sadleir *et al.* 2008). At first glance, this is unexpected, given the evidence for hypercarnivory in *Batrachotomus* documented herein. However, as discussed above, such similitudes suggest a potentially broad diet not reflected in the bite-trace record. *Ticinosuchus*, another Triassic pseudosuchian, is also known to have included fish in its diet (Nesbitt 2011). Thus, *Batrachotomus* and *Ticinosuchus* highlight the potential for a broad dietary spectrum in basal pseudosuchians. In this regard, some regurgitalites including skeletal remains from Vellberg-Eschenau (Schoch & Seegis 2016) could have been produced by *Batrachotomus*, as suggested for Triassic 'rauisuchians', representing another potential behaviour shared with crocodylians (Gordon *et al.* 2020) and further showing conserved feeding ecology in pseudosuchians (Fig. 14). Multidisciplinary studies including bite traces, tooth macrowear and microanatomy, as well as comparisons with taxa with similar dentition, allow for the better identification of feeding habits and ecological roles of extinct taxa. In the same way, studies specifically focused on tooth macrowear and/or microanatomy may already provide information of the feeding ecology of the analysed group (e.g. D'Amore 2009; Brink *et al.* 2015; Wang *et al.* 2015). This is in line with the functionality study of denticulated (ziphodont) teeth by D'Amore (2009). As pointed out in that work, the mesial carina of theropod teeth tend to be less denticulated, suggesting that the mesial carina was used less than the distal carina during feeding. In *Batrachotomus*, this lack of denticles is only observed in the basal portion of the mesial carina of some premaxillary teeth (Fig. 9B; Data S2) and, in contrast to what is observed and expected in theropods (cf. Fiorillo 1991), *Batrachotomus* teeth show higher degrees of abrasion (wear) on the mesial carina (Figs 10, 11), indicating that these parts were more used during feeding. Such wear can be linked to the relatively high frequency of *Knethichnus* (Fig. 8), especially also when this morphotype outlines fan-shaped traces and when it is associated with *Linichnus* in clusters of traces (e.g. Figs 2B, H, 3D, 4K–L). Such traces represent repetitive biting strokes and show changes in the direction of movement of teeth contacting the bone (probably indicating defleshing attempts; see also Feeding ecology and taphonomy, above). *Knethichnus* is a bite trace morphotype exclusively linked to denticulated (ziphodont) teeth (Jacobsen & Bromley 2009) also produced by theropod dinosaurs and *V. komodoensis*. However, in these groups, this bite trace morphotype is much less frequent than others, such as *Nihilichnus* and *Linichnus* (Jacobsen & Bromley 2009; D'Amore & Blumenschine 2009; Drumheller *et al.* 2020). This notable difference is more likely to be explained by different bone usages and feeding behaviours between clades, showing that *Batrachotomus* and pseudosuchians, including extant crocodylians, process the bones more extensively than theropods and *V. komodoensis* (Fig. 14). Fiorillo (1991) noticed that isolated theropod teeth are common in dinosaur fossil localities and that few of them show signs of wear, explaining the low frequency of bone tracing of the clade (and possibly the lack of denticulation of some teeth: D'Amore 2009). Indeed, low levels of tooth wear are in contrast with our findings from the

Batrachotomus tooth assemblage (Figs 9–11; Data S2), including only a few pristine tooth crowns probably corresponding to unerupted teeth. Fiorillo (1991) concluded that theropod dinosaurs did not usually crush bones (potentially with a few exceptions, see Hone & Rauhut 2010) and considered that this ecological role was unoccupied during the Mesozoic. While agreeing with a low level of bone crushing activity by theropods, considering the high frequency of bone tracing by pseudosuchians, we suggest that this ecological role was occupied by the pseudosuchians. Potential evidence for this hypothesis is found in the Lower Cretaceous vertebrate lagerstätte from France analysed by Rozada *et al.* (2021). These authors reported numerous bite traces only associated with crocodylomorphs (see also Gônet *et al.* 2019), even though megalosauroid theropods are also present in the locality (mostly represented by teeth; Rozada *et al.* 2021). Notably, our analysis of archosauromorph teeth shows that those of *Batrachotomus* are mostly similar to those of megalosauroids (Fig. 12; Table 3). Therefore, although *Batrachotomus* and megalosauroids probably shared some feeding habits (see above), it is likely that they also had different ecological roles, again suggesting a broad diet for *Batrachotomus*.

All in all, the relatively lower frequency of bone-tracing by theropods with respect to pseudosuchians (including present-day crocodylians) may relate to different behaviours in the manipulation of prey or carcasses; the former groups would mostly engage in pullback strokes (possibly similar to the behaviour of *V. komodoensis*; e.g. D'Amore 2009; D'Amore & Blumenschine 2009, 2012; Snively *et al.* 2013) resulting in a lower likelihood of tooth–bone contact than that of pseudosuchians (Fig. 14), which usually engage in violent and abrupt moves to tear prey and carcasses (e.g. Drumheller & Brochu 2014, 2016; Njau & Gilbert 2016). Recently, Drumheller *et al.* (2020) documented a bone assemblage with unusually high frequencies of theropod bite traces. These authors linked this to long exposure times for the remains and late access to carcasses (scavenging, including cannibalism) in a stressed ecosystem. Nonetheless, Drumheller *et al.* (2020) also highlighted potential collecting biases against remains with bone surface modifications (see also Pobiner 2008), which could be the case for tyrannosaurs, probably overrepresented in the literature (see also Hone & Rauhut 2010). Even if collecting biases exist in dinosaur localities (as shown by Drumheller *et al.* 2020), in the case of the Lower Keuper, many complete (or nearly complete) bones display bite traces (Figs 3–5; Data S1). This indicates that biases against collection and preparation of incomplete bones do not necessarily preclude the collection of bitten elements, and supports a higher frequency of bone tracing by *Batrachotomus* and pseudosuchians than by theropod dinosaurs, probably resulting from the deep phylogenetic split between these two archosaur clades (Fig. 14).

CONCLUSION

By analysing bite traces on bones produced by the pseudosuchian *Batrachotomus kupferzellensis* together with tooth morphology, microanatomy and macrowear, and comparing them with those of other pseudosuchians (including extinct and extant crocodylians), theropod dinosaurs, and *Varanus komodoensis*, we suggest that phylogeny can be a better predictor of feeding behaviour than tooth morphology (Fig. 14). Even if tooth–bone contact during feeding was mostly unintentional in *Batrachotomus*, as suggested for non-avialan theropods and *V. komodoensis* (Fiorillo 1991; D'Amore & Blumenschine 2009), the high frequency of bitten bones, the predictable distribution of traces within the Lower Keuper assemblage, and the severe damage of many teeth indicate that *Batrachotomus* did not actively avoid such contact. This is comparable to the feeding behaviour of crocodylians (Njau & Gilbert 2016; Shale *et al.* 2017). In this sense, even if bite traces produced by *Batrachotomus* morphologically resemble those of taxa with ziphodont teeth (producing the same ichnotaxa; Jacobsen & Bromley 2009), associations, relative abundances and frequencies of bite traces are more similar to those of the pseudosuchian lineage (Njau & Blumenschine 2006; Noto *et al.* 2012; Boyd *et al.* 2013; Drumheller & Brochu 2014, 2016; Drumheller *et al.* 2014; Njau & Gilbert 2016; Shale *et al.* 2017; Gônet *et al.* 2019; Pujos & Salas-Gismondi 2020; Drymala *et al.* 2021; Rozada *et al.* 2021), a likely synapomorphy of this long-lived hypercarnivorous group. This points to a dichotomy in the interpretation of bite traces: on the one hand, trace morphologies correlate with morphology of teeth and their movement along the bone; on the other hand, the association, location and frequency of bite traces reflect the behaviour of the bite maker, probably differing between carnivorous clades (Fig. 14). Furthermore, our results show that tooth gross morphology alone may not reflect the complete dietary spectrum of a given taxon; this can be overcome by combining analyses of macroscopic wear and microanatomy, which provide independent lines of evidence of dietary preference and feeding behaviour.

Our multidisciplinary analyses of an exceptional association of bite traces, tooth wear patterns, and tooth microanatomy from the Lower Keuper fossil lagerstätten allow the feeding ecology of a 240-million-year-old pseudosuchian reptile to be understood in detail. Despite morphological affinities of *Batrachotomus* teeth with those of megalosauroid theropod dinosaurs, the behaviours

underlying the produced bite traces share greater similarities to those produced by members of the crocodylomorph lineage. This suggests evolutionary conservation of feeding behaviour in this clade, indicating that this successful feeding ecology extended from Triassic pseudosuchians until present-day crocodylians. Concurrently, long-term behavioural and ecological separation between pseudosuchians and theropod dinosaurs was probably the result of the deep phylogenetic split between them.

Acknowledgements. We thank Norbert Adorf, Isabell Rosin, Matthias Boller, Cristina Gascó-Martín, and Marit Kamenz (SMNS) for preparation of specimens and aid on access to specimens, Christoph Wimmer-Pfeil (SMNS) for the preparation of tooth thin sections, and Eli Amson (SMNS) for discussion. We thank Hans Hagdorn (Muschelkalkmuseum, Ingelfingen) for access to specimens and discussion. This research was supported by the Swiss National Science Foundation (PZ00P2_174040) (to CF) and the German Science Foundation (FO 1005/2-1) (to CF). We acknowledge the reviews by an anonymous referee and Domenic C. D'Amore, and the editors David Button and Sally Thomas, who helped to improve a previous version of the manuscript. Open Access funding enabled and organized by Projekt DEAL.

Author contributions. **Conceptualization** E Mujal, C Foth, EE Maxwell, D Seegis, RR Schoch; **Data curation** E Mujal, C Foth, EE Maxwell, D Seegis, RR Schoch; **Formal analysis** E Mujal, C Foth, EE Maxwell; **Funding acquisition** C Foth, RR Schoch; **Investigation** E Mujal, C Foth, EE Maxwell, D Seegis, RR Schoch; **Methodology** E Mujal, C Foth, EE Maxwell; **Project administration** C Foth, RR Schoch; **Resources** C Foth, RR Schoch; **Software** E Mujal, C Foth, EE Maxwell; **Supervision** EE Maxwell, RR Schoch; **Validation** E Mujal, C Foth, EE Maxwell, D Seegis, RR Schoch; **Visualization** E Mujal, C Foth, EE Maxwell, RR Schoch; **Writing – original draft** E Mujal; **Writing – review & editing** E Mujal, C Foth, EE Maxwell, D Seegis, RR Schoch.

DATA ARCHIVING STATEMENT

Data for this study, including Data S1 (bite trace database) and Data S2 (*Batrachotomus* teeth database), are also available in the Dryad Digital Repository: https://doi.org/10.5061/dryad.stqjq2c4b

Editor. David Button

SUPPORTING INFORMATION

Additional Supporting Information can be found online (https://doi.org/10.1111/pala.12597):

Data S1. Database of bite traces on Lower Keuper bones.

Data S2. Database of *Batrachotomus* teeth, with tooth measurements and macroscopic wear.

Appendix S1. Includes Tables S1–S9, which summarize the statistical analysis on bite traces.

REFERENCES

ABEL, O. 1922. Die Schnauzenverletzungen der Parasuchier und ihre biologische Bedeutung. *Paläontologische Zeitschrift*, **5**, 26–57.

ANDERSON, M. J. 2001. A new method for non-parametric multivariate analysis of variance. *Austral Ecology*, **26**, 32–46.

AUGUSTIN, F. J., MATZKE, A. T., MAISCH, M. W. and PFRETZSCHNER, H.-U. 2020. A theropod dinosaur feeding site from the Upper Jurassic of the Junggar Basin, NW China. *Palaeogeography, Palaeoclimatology Palaeoecology*, **560**, 109999.

AVILLA, L. S., FERNANDES, R. and RAMOS, D. F. B. 2004. Bite marks on a crocodylomorph from the Upper Cretaceous of Brazil: evidence of social behavior? *Journal of Vertebrate Paleontology*, **24**, 971–973.

BERTLING, M., BRADDY, S. J., BROMLEY, R. G., DEMATHIEU, G. R., GENISE, J., MIKULÁŠ, R., NIELSEN, J. K., NIELSEN, K. S. S., RINDSBERG, A. K., SCHLIRF, M. and UCHMAN, A. 2006. Names for trace fossils: a uniform approach. *Lethaia*, **39**, 265–286.

BINFORD, L. R. 1981. *Bones: ancient men and modern myths*. Academic Press, 320 pp.

BLUMENSCHINE, R. J., MAREAN, C. W. and CAPALDO, S. D. 1996. Blind tests of inter-analyst correspondence and accuracy in the identification of cut marks, percussion marks, and carnivore tooth marks on bone surfaces. *Journal of Archaeological Science*, **23**, 493–507.

BOYD, C. A., DRUMHELLER, S. K. and GATES, T. A. 2013. Crocodyliform feeding traces on juvenile ornithischian dinosaurs from the Upper Cretaceous (Cenomanian) Kaiparowits Formation, Utah. *PLoS One*, **8**, e57605.

BRINK, K. S., REISZ, R. R., LEBLANC, A. R. H., CHANG, R. S., LEE, Y. C., CHIANG, C. C., HUANG, T. and EVANS, D. C. 2015. Developmental and evolutionary novelty in the serrated teeth of theropod dinosaurs. *Scientific Reports*, **5**, 12338.

BRITT, B. B., EBERTH, D. A., SCHEETZ, R. D., GREENHALGH, B. W. and STADTMAN, K. L. 2009. Taphonomy of debris-flow hosted dinosaur bonebeds at Dalton Wells, Utah (Lower Cretaceous, Cedar Mountain Formation, USA). *Palaeogeography, Palaeoclimatology Palaeoecology*, **280**, 1–22.

BROWN, C., TANKE, M. D. H. and HONE, D. W. E. 2021. Rare evidence for 'gnawing-like' behavior in a small-bodied theropod dinosaur. *PeerJ*, **9**, e11557.

BRUNNER, H. and BRUDER, J. 1981. Standardprofile des Unteren Keupers (Lettenkeuper, Trias) im nördlichen Baden-Württemberg. *Jahresberichte und Mitteilungen des Oberrheinischen Geologische Vereins, N.F*, **63**, 253–269.

BUFFETAUT, E. 1983. Wounds on the jaw of an Eocene mesosuchian crocodilian as possible evidence for the antiquity of crocodilian intraspecific fighting behaviour. *Paläontologische Zeitschrift*, **57**, 143–145.

CHARIG, A. J. and MILNER, A. C. 1997. *Baryonyx walkeri*, a fish-eating dinosaur from the Wealden of Surrey. *Bulletin of the Natural History Museum (Geology Series)*, **53**, 11–70.

COTT, H. B. 1961. Scientific results of an inquiry into the ecology and economic status of the Nile crocodile (*Crocodilus niloticus*) in Uganda and Northern Rhodesia. *Transactions of the Zoological Society of London*, **29**, 211–357.

D'AMORE, D. C. 2009. A functional explanation for denticulation in theropod dinosaur teeth. *The Anatomical Record*, **292**, 1297–1314.

D'AMORE, D. C. and BLUMENSCHINE, R. J. 2009. Komodo monitor (*Varanus komodoensis*) feeding behavior and dental function reflected through tooth marks on bone surfaces, and the application to ziphodont paleobiology. *Paleobiology*, **35**, 525–552.

D'AMORE, D. C. and BLUMENSCHINE, R. J. 2012. Using striated tooth marks on bone to predict body size in theropod dinosaurs: a model based on feeding observations of *Varanus komodoensis*, the Komodo monitor. *Paleobiology*, **38**, 79–100.

DE VITA, D. E. 1979. Niche separation and the broken-stick model. *The American Naturalist*, **114**, 171–178.

DRUMHELLER, S. K. and BROCHU, C. A. 2014. A diagnosis of *Alligator mississippiensis* bite marks with comparisons to existing crocodylian datasets. *Ichnos*, **21**, 131–146.

DRUMHELLER, S. K. and BROCHU, C. A. 2016. Phylogenetic taphonomy: a statistical and phylogenetic approach for exploring taphonomic patterns in the fossil record using crocodylians. *Palaios*, **31**, 463–478.

DRUMHELLER, S. K., McHUGH, J. B., KANE, M., RIEDEL, A. and D'AMORE, D. C. 2020. High frequencies of theropod bite marks provide evidence for feeding, scavenging, and possible cannibalism in a stressed Late Jurassic ecosystem. *PLoS One*, **15**, e0233115.

DRUMHELLER, S. K., STOCKER, M. R. and NESBITT, S. J. 2014. Direct evidence of trophic interactions among apex predators in the Late Triassic of western North America. *Naturwissenschaften*, **101**, 975–987.

DRYMALA, S. M., BADER, K. and PARKER, W. G. 2021. Bite marks on an aetosaur (Archosauria, Suchia) osteoderm: assessing Late Triassic predator-prey ecology through ichnology and tooth morphology. *Palaios*, **36**, 28–37.

ETZOLD, A. and SCHWEIZER, V. 2005. Der Keuper in Baden-Württemberg. 215–258. *In* DEUTSCHE STRATIGRAPHISCHE KOMMISSION (eds). *Stratigraphie von Deutschland IV. Keuper. Bearbeitet von der Arbeitsgruppe Keuper der Subkommission Perm-Trias der DSK*. Courier Forschungsinstitut Senckenberg, 253 pp.

FIORILLO, A. R. 1991. Prey bone utilization by predatory dinosaurs. *Palaeogeography, Palaeoclimatology Palaeoecology*, **88**, 157–166.

FRANÇA, M. A. G., FERIGOLO, J. and LANGER, M. C. 2011. Associated skeletons of a new Middle Triassic "Rauisuchia" from Brazil. *Naturwissenschaften*, **98**, 389–395.

GIGNAC, P. M. and ERICKSON, G. M. 2017. The biomechanics behind extreme osteophagy in *Tyrannosaurus rex*. *Scientific Reports*, **7**, 2012.

GÔNET, J., ROZADA, L., BOURGEAIS, R. and ALLAIN, R. 2019. Taphonomic study of a pleurosternid turtle shell from the Early Cretaceous of Angeac-Charente, southwest France. *Lethaia*, **52**, 232–243.

GORDON, C. M., ROACH, B. T., PARKER, W. G. and BRIGGS, D. E. G. 2020. Distinguishing regurgitalites and coprolites: a case study using a Triassic bromalite with soft tissue of the pseudosuchian archosaur *Revueltosaurus*. *Palaios*, **35**, 111–121.

GOWER, D. J. 1999. The cranial and mandibular osteology of a new rauisuchian archosaur from the Middle Triassic of southern Germany. *Stuttgarter Beiträge zur Naturkunde. Serie B (Geologie und Paläontologie)*, **280**, 1–49.

GOWER, D. J. and SCHOCH, R. R. 2009. The postcranial skeleton of the rauisuchian *Batrachotomus kupferzellensis*. *Journal of Vertebrate Paleontology*, **29**, 103–122.

HAGDORN, H., SCHOCH, R. R., SEEGIS, D. and WERNEBURG, R. 2015. Wirbeltierlagerstätten im Lettenkeuper. 325–358. *In* HAGDORN, H., SCHOCH, R. R. and SCHWEIGERT, G. (eds). *Der Lettenkeuper – Ein Fenster in die Zeit vor den Dinosauriern*. Staatliches Museum für Naturkunde Stuttgart.

HAMMER, Ø. 2020. PAST: PAleontological STatistics. Version 4.03. Reference manual. University of Oslo, Oslo. https://www.nhm.uio.no/english/research/infrastructure/past/

HAMMER, Ø. and HARPER, D. A. T. 2006. *Paleontological data analysis*. Blackwell Publishing, 351 pp.

HAMMER, Ø., HARPER, D. A. T. and RYAN, P. D. 2001. PAST: paleontological statistics software package for education and data analysis. *Palaeontologia Electronica*, **4**, 1–9.

HENDRICKX, C., MATEUS, O. and ARAÚJO, R. 2015. The dentition of megalosaurid theropods. *Acta Palaeontologica Polonica*, **60**, 627–642.

HOFFMAN, D. K., EDWARDS, H. R., BARRETT, P. M. and NESBITT, S. J. 2019. Reconstructing the archosaur radiation using a Middle Triassic archosauriform tooth assemblage from Tanzania. *PeerJ*, **7**, e7970.

HONE, D. W. E. and CHURE, D. J. 2018. Difficulties in assigning trace makers from theropodan bite marks: an example from a young diplodocoid sauropod. *Lethaia*, **51**, 456–466.

HONE, D. W. E. and RAUHUT, O. W. M. 2010. Feeding behaviour and bone utilization by theropod dinosaurs. *Lethaia*, **43**, 232–244.

HUNGERBÜHLER, A. 1998. Taphonomy of the prosauropod dinosaur *Sellosaurus*, and its implications for carnivore faunas and feeding habits in the Late Triassic. *Palaeogeography, Palaeoclimatology Palaeoecology*, **143**, 1–29.

JACKSON, D. A. 1993. Stopping rules in principal components analysis: a comparison of heuristical and statistical approaches. *Ecology*, **74**, 2204–2214.

JACOBSEN, A. R. 1998. Feeding behaviour of carnivorous dinosaurs as determined by tooth marks on dinosaur bones. *Historical Biology*, **13**, 17–26.

JACOBSEN, A. R. and BROMLEY, R. G. 2009. New ichnotaxa based on tooth impressions on dinosaur and whale bones. *Geological Quarterly*, **53**, 373–382.

KÄLIN, J. A. 1936. Über Skelettanomalien bei Crocodiliden. *Zeitschrift für Morphologie und Oekologie der Tiere*, **32**, 327–347.

KATSURA, Y. 2004. Paleopathology of *Toyotamaphimeia machikanensis* (Diapsida, Crocodylia) from the Middle Pleistocene of Central Japan. *Historical Biology*, **16**, 93–97.

KLEIN, N., FOTH, C. and SCHOCH, R. R. 2017. Preliminary observations on the bone histology of the Middle Triassic pseudosuchian archosaur *Batrachotomus kupferzellensis* reveal fast growth with laminar fibrolamellar bone tissue. *Journal of Vertebrate Paleontology*, **37**, e1333121.

LONGRICH, N. R., HORNER, J. H., ERICKSON, G. M. and CURRIE, P. J. 2010. Cannibalism in *Tyrannosaurus rex*. *PLoS One*, **5**, e13419.

MARSH, A. D. and ROWE, T. B. 2020. A comprehensive anatomical and phylogenetic evaluation of *Dilophosaurus wetherilli* (Dinosauria, Theropoda) with descriptions of new specimens from the Kayenta Formation of northern Arizona. *Journal of Paleontology*, **94**, 1–103.

MIKULÁŠ, R., KADLECOVÁ, E., FEJFAR, O. and DVOŘÁK, Z. 2006. Three new ichnogenera of biting and gnawing traces on reptilian and mammalian bones: a case study from the Miocene of the Czech Republic. *Ichnos*, **13**, 113–127.

MUJAL, E. and SCHOCH, R. R. 2020. Middle Triassic (Ladinian) amphibian tracks from the Lower Keuper succession of southern Germany: Implications for temnospondyl locomotion and track preservation. *Palaeogeography, Palaeoclimatology Palaeoecology*, **543**, 109625.

MUJAL, E., FOTH, C., MAXWELL, E. E., SEEGIS, D. and SCHOCH, R. R. 2022. Data from: Feeding habits of the Middle Triassic pseudosuchian *Batrachotomus kupferzellensis* from Germany and palaeoecological implications for archosaurs. *Dryad Digital Repository*. https://doi.org/10.5061/dryad.stqjq2c4b

NESBITT, S. J. 2011. The early evolution of archosaurs: relationships and the origin of major clades. *Bulletin of the American Museum of Natural History*, **352**, 1–292.

NESBITT, S. J., BRUSATTE, S. L., DESOJO, J. B., LIPARINI, A., DE FRANÇA, M. A. G., WEINBAUM, J. C. and GOWER, D. 2013. Rauisuchia. 241–274. *In* NESBITT, S. J., DESOJO, J. B. and IRMIS, R. B. (eds). *Anatomy, phylogeny and palaeobiology of early archosaurs and their kin*. Geological Society, London, Special Publications, **379**.

NESBITT, S. J., ZAWISKIE, J. M. and DAWLEY, R. M. 2020. The osteology and phylogenetic position of the loricatan (Archosauria: Pseudosuchia) *Heptasuchus clarki*, from the ? Mid-Upper Triassic, southeastern Big Horn Mountains, Central Wyoming (USA). *PeerJ*, **8**, e10101.

NIEDŹWIEDZKI, G., GORZELAK, P. and SULEJ, T. 2011. Bite traces on dicynodont bones and the early evolution of large terrestrial predators. *Lethaia*, **44**, 87–92.

NITSCH, E. 2015*a*. Der Lettenkeuper – Verbreitung, Alter, Paläogeographie. 9–16. *In* HAGDORN, H., SCHOCH, R. R. and SCHWEIGERT, G. (eds). *Der Lettenkeuper – Ein Fenster in die Zeit vor den Dinosauriern*. Staatliches Museum für Naturkunde Stuttgart.

NITSCH, E. 2015*b*. Lithostratigraphie des Lettenkeupers. 27–40. *In* HAGDORN, H., SCHOCH, R. R. and SCHWEIGERT, G. (eds). *Der Lettenkeuper – Ein Fenster in die Zeit vor den Dinosauriern*. Staatliches Museum für Naturkunde Stuttgart.

NITSCH, E. 2015*c*. Fazies und Ablagerungsräume des Lettenkeupers. 285–324. *In* HAGDORN, H., SCHOCH, R. R. and SCHWEIGERT, G. (eds). *Der Lettenkeuper – Ein Fenster in die Zeit vor den Dinosauriern*. Staatliches Museum für Naturkunde Stuttgart.

NJAU, J. K. and BLUMENSCHINE, R. J. 2006. A diagnosis of crocodile feeding traces on larger mammal bone, with fossil examples from the Plio-Pleistocene Olduvai Basin, Tanzania. *Journal of Human Evolution*, **50**, 142–162.

NJAU, J. K. and GILBERT, H. G. 2016. A taxonomy for crocodile-induced bone modifications and their relevance to paleoanthropology. *FOROST Occasional Publications*, **3**, 1–13.

NOTO, C. R., MAIN, D. J. and DRUMHELLER, S. K. 2012. Feeding traces and paleobiology of a Cretaceous (Cenomanian) crocodyliform: example from the Woodbine Formation of Texas. *Palaios*, **27**, 105–115.

PIRRONE, C. A., BUATOIS, L. A. and BROMLEY, R. G. 2014. Ichnotaxobases for bioerosion trace fossils in bones. *Journal of Paleontology*, **88**, 195–203.

POBINER, B. 2008. Paleoecological information in predator tooth marks. *Journal of Taphonomy*, **6**, 373–397.

PUJOS, F. and SALAS-GISMONDI, R. 2020. Predation of the giant Miocene caiman *Purussaurus* on a mylodontid ground sloth in the wetlands of proto-Amazonia. *Biology Letters*, **16**, 20200239.

QVARNSTRÖM, M., AHLBERG, P. E. and NIEDŹWIEDZKI, G. 2019. Tyrannosaurid-like osteophagy by a Triassic archosaur. *Scientific Reports*, **9**, 925.

ROGERS, R. R., KRAUSE, D. W. and ROGERS, K. C. 2003. Cannibalism in the Madagascan dinosaur *Majungatholus atopus*. *Nature*, **422**, 515–518.

ROZADA, L., ALLAIN, R., VULLO, R., GOEDERT, J., AUGIER, D., JEAN, A., MARCHAL, J., PEYRE DE FABRÈGUES, C., QVARNSTRÖM, M. and ROYO-TORRES, R. 2021. A Lower Cretaceous *Lagerstätte* from France: a taphonomic overview of the Angeac-Charente vertebrate assemblage. *Lethaia*, **54**, 141–165.

SADLEIR, R., BARRETT, P. M. and POWELL, H. P. 2008. The anatomy and systematics of *Eustreptospondylus oxoniensis*, a theropod dinosaur from the Middle Jurassic of Oxfordshire, England. *Palaeontographical Society Monograph London*, **160**, 1–82.

SANDER, P. M. 1999. The microstructure of reptilian tooth enamel: terminology, function, and phylogeny. *Münchner Geowissenschaftliche Abhandlungen A*, **38**, 1–102.

SCHOCH, R. R. 1999. Comparative osteology of *Mastodonsaurus giganteus* (Jaeger, 1828) from the Middle Triassic (Lettenkeuper: Longobardian) of Germany (Baden-Württemberg, Bayern, Thüringen). *Stuttgarter Beiträge zur Naturkunde. Serie B (Geologie und Paläontologie)*, **278**, 1–175.

SCHOCH, R. R. and MILNER, A. R. 2000. *Handbuch der Paläoherpetologie 3B: Stereospondyli*. F. Pfeil, 203 pp.

SCHOCH, R. R. and SEEGIS, D. 2016. A Middle Triassic palaeontological gold mine: the vertebrate deposits of Vellberg (Germany). *Palaeogeography, Palaeoclimatology Palaeoecology*, **459**, 249–267.

SCHOCH, R. R., ULLMANN, F., ROZYNEK, B., ZIEGLER, R., SEEGIS, D. and SUES, H.-D. 2018. Tetrapod diversity and palaeoecology in the German Middle Triassic (Lettenkeuper) documented by tooth morphotypes. *Palaeobiodiversity & Palaeoenvironments*, **98**, 615–638.

SCHUBERT, B. W. and UNGAR, P. S. 2005. Wear facets and enamel spalling in tyrannosaurid dinosaurs. *Acta Palaeontologica Polonica*, **50**, 93–99.

SHALE, Y., EL ZAATARI, S. and WHITE, T. D. 2017. Hominid butchers and biting crocodiles in the African Plio–Pleistocene. *Proceedings of the National Academy of Sciences*, **114**, 13164–13169.

SMITH, J. B., VANN, D. R. and DODSON, P. 2005. Dental morphology and variation in theropod dinosaurs: implications for the taxonomic identification of isolated teeth. *The Anatomical Record*, **285A**, 699–736.

SNIVELY, E., COTTON, J. R., RIDGELY, R. C. and WITMER, L. M. 2013. Multibody dynamics model of head and neck function in *Allosaurus* (Dinosauria, Theropoda). *Palaeontologia Electronica*, **16**, 11A.

STEHMAN, S. V. 1997. Selecting and interpreting measures of thematic classification accuracy. *Remote Sensing of Environment*, **62**, 77–89.

URLICHS, M. 1982. Zur Stratigraphie und Fossilführung des Lettenkeupers (Ob. Trias) bei Schwäbisch Hall (Baden-Württemberg). *Jahresberichte und Mitteilungen des Oberrheinischen Geologische Vereins, N.F*, **64**, 213–224.

VALLON, L. H., RINDSBERG, A. K. and MARTIN, A. J. 2015. The use of the terms trace, mark and structure. *Annales Societatis Geologorum Poloniae*, **85**, 527–528.

WANG, C.-C., SONG, Y.-F., SONG, S.-R., JI, Q., CHIANG, C.-C., MENG, Q., LI, H., HSIAO, K., LU, Y.-C., SHEW, B.-Y., HUANG, T. and REISZ, R. R. 2015. Evolution and function of dinosaur teeth at ultramicrostructural level revealed using synchrotron transmission X-ray microscopy. *Scientific Reports*, **5**, 15202.

WEBB, G. J. W. and MANOLIS, S. C. 1983. *Crocodylus johnstoni* in the McKinlay river area, N.T.V.* Abnormalities and injuries. *Australian Wildlife Research*, **10**, 407–420.

WHITNEY, M. R., LEBLANC, A. R. H., REYNOLDS, A. R. and BRINK, K. S. 2020. Convergent dental adaptations in the serrations of hypercarnivorous synapsids and dinosaurs. *Biology Letters*, **16**, 20200750.

WILD, R. 1978. Massengrab für Saurier. *Kosmos*, **11**, 790–797.

WILD, R. 1979. Saurier kommen ans Licht. *Tierwelt*, **4**, 38–45.

WILD, R. 1980. The fossil deposits of Kupferzell, Southwest Germany. *Mesozoic Vertebrate Life*, **1**, 15–18.

WILLS, M. A., BRIGGS, D. E. G. and FORTEY, R. A. 1994. Disparity as an evolutionary index: a comparison of Cambrian and recent arthropods. *Paleobiology*, **20**, 93–130.

YOUNG, M. T., BRUSATTE, S. L., BEATTY, B. L., ANDRADE, M. B. and DESOJO, J. B. 2012. Tooth-on-tooth interlocking occlusion suggests macrophagy in the Mesozoic marine crocodylomorph *Dakosaurus*. *The Anatomical Record*, **295**, 1147–1158.